HHS Public Access

Author manuscript

Nat Rev Cardiol. Author manuscript; available in PMC 2023 March 03.

Published in final edited form as:

Nat Rev Cardiol. 2022 October ; 19(10): 684–703. doi:10.1038/s41569-022-00687-9.

Addresses for correspondence: Ik-Kyung Jang, MD, PhD, Allan and Gill Gray Professor of Medicine, Harvard Medical School, Cardiology Division, Massachusetts General Hospital, 55 Fruit Street | GRB 800 | Boston, MA 02114, USA, Tel: +1-617-726-9226; Fax: +1-617-726-7419, ijang@mgh.harvard.edu.

*All coauthors are listed at the end of the text.

Disclosure

Dr. Adriaenssens received educational grants from Abbott Vascular. Dr. Aguirre received research grants from Philips Healthcare, Inc. and Amgen, Inc. Dr. Akasaka received research grants from Abbott Vascular Japan, Nipro Inc., and Terumo Inc. and is a medical advisor for Terumo Inc. Dr. Ali: institutional grants from Abbott vascular, and cardiovascular system Inc. to Columbia University and Cardiovascular Research foundation; honoraria from Amgen, Astra Zeneca, Boston scientific; equity from Shockwave. Dr. Amabile received proctoring and consulting fees for Abbott Vascular & Boston Scientific; consulting fees for Shockwave Medical; institutional research grants from Abbott Vascular. Dr. Arbustini received grants from the Ministry of Health to the National IRCCS Cardiology Network (RCR-2019-23669116-001 and RCR-2020-23670065) and from FRRB grant CP_14/2018, INTESTRAT-CAD, Lombardia Region, Italy. Dr. Bouma has OCT patents, assigned to Massachusetts General Hospital and licensed to Terumo Corporation. Dr. Crea received personal fees from Amgen, personal fees from Astra Zeneca, personal fees from Servier, personal fees from BMS, other from GlyCardial Diagnostics, outside the submitted work. Dr. Dauerman is a consultant to Baim Clinical Research Institute, Cardiovascular Research Foundation, Medtronic and Boston Scientific; Dr. Dauerman has research grants from Medtronic and Boston Scientific. Dr. Di Mario received research grants (to the institution) from AMGEN, Behring, Boston Scientific, Chiesi, Daiichi-Sankyo, Edwards, Medtronic, Shockwave Volcano-Philips and speakers' fees from Abbott and Shockwave. Dr. Finn and Dr. Virmani received institutional research support from NIH (HL141425), Leducq Foundation Grant; 480 Biomedical; 4C Medical; 4Tech; Abbott; Accumedical; Amgen; Biosensors; Boston Scientific; Cardiac Implants; Celonova; Claret Medical; Concept Medical; Cook; CSI; DuNing, Inc; Edwards LifeSciences; Emboline; Endotronix; Envision Scientific; Lutonix/Bard; Gateway; Lifetech; Limflo; MedAlliance; Medtronic; Mercator; Merill; Microport Medical; Microvention; Mitraalign; Mitra assist; NAMSA; Nanova; Neovasc; NIPRO; Novogate; Occulotech; OrbusNeich Medical; Phenox; Profusa; Protembis; Qool; Recor; Senseonics; Shockwave; Sinomed; Spectranetics; Surmodics; Symic; Vesper; W.L. Gore; Xeltis. A.V.F. has received honoraria from Abbott Vascular; Biosensors; Boston Scientific; Celonova; Cook Medical; CSI; Lutonix Bard; Sinomed; Terumo Corporation; and is a consultant to Amgen; Abbott Vascular; Boston Scientific; Celonova; Cook Medical; Lutonix Bard; Sinomed. R.V. has received honoraria from Abbott Vascular; Biosensors; Boston Scientific; Celonova; Cook Medical; Cordis; CSI; Lutonix Bard; Medtronic; OrbusNeich Medical; CeloNova; SINO Medical Technology; ReCore; Terumo Corporation; W. L. Gore; Spectranetics; and is a consultant Abbott Vascular; Boston Scientific; Celonova; Cook Medical; Cordis; CSI; Edwards Lifescience; Lutonix Bard; Medtronic; OrbusNeich Medical; ReCore; Sinomededical Technology; Spectranetics; Surmodics; Terumo Corporation; W. L. Gore; Xeltis. Dr. Fujimoto has financial interests in Optovue, receives royalties from intellectual property owned by MIT and licensed to Optovue and receives research support from Topcon and the National Institutes of Health. Dr. Garcia-Garcia recieved institutional grant support: Biotronik, Boston Scientific, Medtronic, Abbott, Neovasc, Shockwave, Philips, and CorFlow. Dr. Gerbaud is a consultant for Terumo and Abbott Vascular. Dr. Gonzalo received speaker and consultant fees from Abbott, speaker fees from Boston Scientific. Dr. Gori received speakeŕs honoraria and research support from Abbot vascular. Dr. Guagliumi received consultant fees from Abbott Vascular and Infraredx; research grant from Abbott Vascular, Infraredx, and Amgen. Dr. Hibi has received remuneration for lectures from Terumo, Abbott Vascular, and Boston Scientific Japan. Dr. Holm received speaker fees from Terumo, research grants and speaker fees from Abbott and Reva Medical, research grants from Boston Scientific, Biosensors, Bbraun, and Medis Medical Imaging. Dr. Jang received educational grants from Abbott Vascular and consulting fees from Svelte and Mitobridge. Dr. Jung-Sun Kim received proctoring fees from Abbott Vascular. Dr. Libby is an unpaid consultant to, or involved in clinical trials for Amgen, AstraZeneca, Baim Institute, Beren Therapeutics, Esperion Therapeutics, Genentech, Kancera, Kowa Pharmaceuticals, Medimmune, Merck, Norvo Nordisk, Novartis, Pfizer, Sanofi-Regeneron. Dr. Libby is a member of scientific advisory board for Amgen, Caristo, Cartesian, Corvidia Therapeutics, CSL Behring, DalCor Pharmaceuticals, Dewpoint, Kowa Pharmaceuticals, Olatec Therapeutics, Medimmune, Novartis, PlaqueTec, and XBiotech, Inc. Dr. Kume received personal fees from Abbott Japan Co., Ltd. Dr. Libby's laboratory has received research funding in the last 2 years from Novartis. Dr. Libby is on the Board of Directors of XBiotech, Inc. Dr. Libby has a financial interest in Xbiotech, a company developing therapeutic human antibodies. Dr. Libby's interests were reviewed and are managed by Brigham and Women's Hospital and Partners HealthCare in accordance with their conflict-of-interest policies. Dr. Libby's laboratory has received research funding in the last 2 years from Novartis. Dr. Libby is on the Board of Directors of XBiotech, Inc. Dr. Libby has a financial interest in Xbiotech, a company developing therapeutic human antibodies. Dr. Libby's interests were reviewed and are managed by Brigham and Women's Hospital and Partners HealthCare in accordance with their conflict-of-interest policies. Dr. Johnson received consultancy and speaker fees from Abbott Vascular & Terumo. Dr. Joner reports personal fees from Biotronik, personal fees from Orbus Neich, grants and personal fees from Boston Scientific, grants and personal fees from Edwards, personal fees from Recor, personal fees from Astra Zeneca, grants from Amgen, personal fees from Abbott, personal fees from Shockwave, grants from Infraredx, grants from Cardiac Dimensions outside the submitted work. Dr. Lerman received consultant fees from Volcano and Philips. Dr. Michalis received departmental grants from Abbott. Dr. Minami received an honorarium and consulting fee from Abbott. Dr. Mintz received honoraria from Boston Scientific, Philips/Volcano, Medtronic, Abiomed. Equity in SpectraWave. Dr. Nef received speaker honoraria and research grant from Abbott Vascular. Dr. Räber received grants to the institution by Abbott, Biotronik, BostonScientific, Heartflow, Sanofi, Regeneron and speaker/consultation fees by Abbott, Amgen, AstraZeneca, Canon, Occlutec, Sanofi, Vifor. Dr. Regar is a member of the medical advisory board for Zed Medical, Inc. and a clinical advisor for Kaminari Medical BV. Dr. Reynolds received donations for research from Abbott vascular, Siemens, and BioTelemetry. Dr. Shinke received research grant from Abbott Medical Japan. Dr. Souteyrand received consulting for Abbott medical, Terumo, Boston scientific, Medtronic, Schockwave. Dr. Stone received speaker honoraria from Terumo, Cook, Infraredx; consultant to Valfix, TherOx, Robocath, HeartFlow,

Optical coherence tomography in coronary atherosclerosis

Ablative Solutions, Vectorious, Miracor, Neovasc, Abiomed, Ancora, Elucid Bio, Occlutech, CorFlow, Reva, MAIA Pharmaceuticals, Vascular Dynamics, Shockwave, V-Wave, Cardiomech, Gore; equity/options from Ancora, Cagent, Applied Therapeutics, Biostar family of funds, SpectraWave, Orchestra Biomed, Aria, Cardiac Success, Valfix, MedFocus family of funds. Dr. Tearney receives sponsored research funding from Canon, CN USA Biotech Holdings, VivoLight and AstraZeneca and catheter materials from Terumo Corporation. Dr. Tearney has a financial/fiduciary interest in SpectraWave, a company developing an OCT-NIRS intracoronary imaging system and catheter. His financial/fiduciary interest was reviewed and is managed by the Massachusetts General Hospital and Mass General Brigham HealthCare in accordance with their conflict of interest policies. Dr. Tearney (Terumo, Canon, Spectrawave) has the right to receive royalties from licensing arrangements. Dr. Toutouzas received research grants from Medtronic, and I am proctor for Medtronic and Abbott. Dr. Uemura received educational grants from Abbott Vascular Japan. Dr. Vergallo received speaker fees from Abbott. Dr. Weisz is a member of medical advisory board for Filterlex, Intratech, Microbot, and Trisol and received equity from Filterlex, Intratech, and Microbot and consulting fees from Filterlex, Intratech, Microbot, Magenta, and Cuspa. Dr. William: institutional research grant and honoraria from MicroPort (steering Committee TARGET AC trial; co-founder Argonauts, an innovation facilitator; medical advisor Rede Optimus Research and Corrib Core Laboratory, NUI Galway. Dr. Yan received research grant and speaker honorarium from Abbott Vascular. Dr. Yonetsu received endowment from Abbott Vascular Japan, Boston Scientific Japan, WIN International, Japan Lifeline, and Takeyama KK. Dr. Yu received research grants from the National Key R&D Program of China (2016YFC1301103) and the National Natural Science Foundation of China (81827806). The other writing committee members and coauthors declare that there is no conflict of interest.

Coauthors

Aguirre, Aaron D; Akasaka, Takashi; Arbab-Zadeh, Armin; Arbustini, Eloisa; Bouma, Brett; Bryniarski, Krzysztof L.; Chen, Yundai; Croce, Kevin; Daemen, Joost; Di Vito, Luca; Dijkstra, Jouke; Farb, Andrew; Finn, Aloke V.; Fracassi, Francesco; Garcia-Garcia, Hector M.; Gerbaud, Edouard; Gili, Sebastiano; Gori, Tommaso; Granada, Juan F.; Hibi, Kiyoshi; Higuma, Takumi; Iannaccone, Mario; Jang, Yangsoo; Kim, Hyung Oh; Kimura, Shigeki; Kini, Annapoorna S.; Kubo, Takashi; Kume, Teruyoshi; Kurihara, Osamu; Lee, Tetsumin; Lerman, Amir; Libby, Peter; Michalis, Lampros K.; Montone, Rocco A.; Nakajima, Akihiro; Nakamura, Sunao; Narula, Jagat; Niccoli, Giampaolo; Nishimiya, Kensuke; Opolski, Maksymilian P.; Papafaklis, Michail I.; Park, Seung-Jung; Pinto, Fausto; Prasad, Abhiram; Regar, Evelyn; Reynolds, Harmony; Russo, Michele; Saito, Yoshihiko; Sankardas, Mullasari Ajit; Saw, Jacqueline; Shimokawa, Hiroaki; Soeda, Tsunenari; Subban, Vijayakumar; Sugiyama, Tomoyo; Takano, Masamichi; Tanaka, Atsushi; Tearney, Guillermo J.; Thondapu, Vikas; Toutouzas, Konstantinos; Virmani, Renu; Weissman, Neil J.; Wijns, William; Yamamoto, Erika; Yan, Bryan P.; Yasuda, Satoshi; Ye, Jong Chul; Yu, Bo

Affiliations of coauthors

Aguirre, Aaron: Massachusetts General Hospital, Boston, Massachusetts, USA
Akasaka, Takashi: Wakayama Medical University, Wakayama, Japan
Arbab-Zadeh, Armin: Johns Hopkins University, Baltimore, Maryland, USA
Arbustini, Eloisa: IRCCS Foundation University Hospital Policlinico San Matteo, Pavia, Italy
Bouma, Brett: Massachusetts General Hospital, Boston, Massachusetts, USA
Bryniarski, Krzysztof L.: Jagiellonian University Medical College, Institute of Cardiology, Department of Interventional Cardiology, John Paul II Hospital, Krakow, Poland
Chen, Yundai: Sixth Medical Center, Chinese PLA General Hospital, Beijing, China
Croce, Kevin: Brigham and Women's Hospital, Boston, Massachusetts, USA
Daemen, Joost: Erasmus University Medical Centre, Rotterdam, The Netherlands
Di Vito, Luca: Mazzoni Hospital, Ascoli Piceno, Italy
Dijkstra, Jouke: Leiden University Medical Centre, Leiden, the Netherlands
Farb, Andrew: Food and Drug Administration, Silver Spring, Maryland, USA
Finn, Aloke V.: CV Path Institute, Gaithersburg, Maryland, USA
Fracassi, Francesco: Catholic University of the Sacred Heart, Rome, Italy; Vigevano Civil Hospital, ASST Pavia, Italy
Garcia-Garcia, Hector M.: MedStar Washington Hospital Center, Washington, D.C., USA
Gerbaud, Edouard: University Hospital of Bordeaux, Pessac, France
Gili, Sebastiano: Centro Cardiologico Monzino, IRCCS, Milan, Italy
Gori, Tommaso: Universitätsmedizin Mainz and DZHK Rhein-Main, Germany
Granada, Juan F.: Cardiovascular Research Foundation, New York, New York, USA
Hibi, Kiyoshi: Yokohama City University Medical Center, Kanagawa, Japan
Higuma, Takumi: Kawasaki Municipal Tama Hospital, St. Marianna University School of Medicine, Kanagawa, Japan
Iannaccone, Mario: Ospedale San Giovanni Bosco, Turin, Italy
Jang, Yangsoo: Yonsei University College of Medicine, Seoul, South Korea
Kim, Hyung Oh: Kyung Hee University, Seoul, South Korea
Kimura, Shigeki: Yokohama Minami Kyosai Hospital, Kanagawa, Japan
Kini, Annapoorna S.: Mount Sinai Hospital, New York, New York, USA
Kubo, Takashi: Wakayama Medical University, Wakayama, Japan
Kume, Teruyoshi: Kawasaki Medical School, Okayama, Japan
Kurihara, Osamu: Nippon Medical School Chiba Hokusoh Hospital, Chiba, Japan
Lee, Tetsumin: Japanese Red Cross Musashino Hospital, Tokyo, Japan
Lerman, Amir: Mayo Clinic, Rochester, Minnesota, USA
Libby, Peter: Brigham and Women's Hospital, Boston, Massachusetts, USA
Michalis, Lampros K.: University of Ioannina Medical School, Ioannina, Greece

assessment and intervention

Makoto Araki[1], **Carlo Di Mario**[2], **Giulio Guagliumi**[3], **Adnan Kastrati**[4], **Javier Escaned**[5], **Michael Joner**[6], **Thomas W. Johnson**[7], **Lorenz Räber**[8], **Tom Adriaenssens**[9], **Francesco Prati**[10], **Holger Nef**[11], **Harold L. Dauerman**[12], **Marc Feldman**[13], **Gregg W. Stone**[14], **Giora Weisz**[15], **Ron Waksman**[16], **Akiko Maehara**[17], **Ziad Ali**[17], **Nicolas Amabile**[18], **Geraud Souteyrand**[19], **Nicolas Meneveau**[20], **Niels Holm**[21], **Fernando Alfonso**[22], **Nieves Gonzalo**[23], **Rocco Vergallo**[24], **Jung-Sun Kim**[25], **Myeong-Ki Hong**[25], **O. Christopher Raffel**[26], **Peter Barlis**[27], **Gary S. Mintz**[17], **Christos V. Bourantas**[28], **Taishi Yonetsu**[29], **Yoshiyasu Minami**[30], **Toshiro Shinke**[31], **Shiro Uemura**[32], **Tsunekazu Kakuta**[33], **James Fujimoto**[34], **Valentin Fuster**[14], **Filippo Crea**[24], **Ik-Kyung Jang, MD, PhD**[1]

[1]Massachusetts General Hospital, Boston, Massachusetts, USA

[2]Careggi University Hospital, Florence, Italy

[3]Ospedale Papa Giovanni XXIII, Bergamo, Italy

[4]Technische Universität München, München, Germany, and Munich Heart Alliance, Munich, Germany

---

Montone, Rocco A.: Catholic University of the Sacred Heart, Rome, Italy.
Nakajima, Akihiro: Massachusetts General Hospital, Boston, Massachusetts, USA
Nakamura, Sunao: New Tokyo Hospital, Chiba, Japan
Narula, Jagat: Icahn School of Medicine at Mount Sinai, New York, New York, USA
Niccoli, Giampaolo: Catholic University of the Sacred Heart, Rome, Italy
Nishimiya, Kensuke: Tohoku University Graduate School of Medicine, Sendai, Japan
Opolski, Maksymilian P.: National Institute of Cardiology, Warsaw, Poland
Papafaklis, Michail I.: University Hospital of Ioannina, Ioannina, Greece
Park, Seung-Jung: Asan Medical Center, Seoul, South Korea
Pinto, Fausto: Santa Maria University Hospital, CHULN Center of Cardiology of the University of Lisbon, Lisbon School of Medicine, Lisbon Academic Medical Center, Lisboa, Portugal
Prasad, Abhiram: Mayo Clinic, Rochester, Minnesota, USA
Regar, Evelyn: University Hospital Zürich, Zürich, Switzerland
Reynolds, Harmony: New York University Grossman School of Medicine, New York, NY
Russo, Michele: Catholic University of the Sacred Heart, Rome, Italy; S. Maria delle Croci Hospital, Ravenna, Italy
Saito, Yoshihiko: Gifu University Graduate School of Medicine, Gifu, Japan
Sankardas, Mullasari Ajit: Madras Medical Mission, Chennai, India
Saw, Jacqueline: Vancouver General Hospital, University of British Columbia, Canada
Shimokawa, Hiroaki: International University of Health and Welfare, Chiba, Japan
Soeda, Tsunenari: Nara Medical University, Nara, Japan
Subban, Vijayakumar: Madras Medical Mission, Chennai, India
Sugiyama, Tomoyo: Tsuchiura Kyodo General Hospital, Ibaraki, Japan
Takano, Masamichi: Nippon Medical School Chiba Hokusoh Hospital, Chiba, Japan
Tanaka, Atsushi: Wakayama Medical University, Wakayama, Japan
Tearney, Guillermo J.: Massachusetts General Hospital, Boston, Massachusetts, USA
Thondapu, Vikas: Massachusetts General Hospital, Boston, Massachusetts, USA
Toutouzas, Konstantinos: National and Kapodistrian University of Athens, Athens, Greece
Virmani, Renu: CVPath Institute, Gaithersburg, Maryland, USA
Weissman, Neil J.: MedStar Health Research Institute, Washington, DC, USA
Wijns, William: National University of Ireland Galway and Saolta University Healthcare Group, Galway, Ireland
Yamamoto, Erika: Kyoto University Graduate School of Medicine, Kyoto, Japan
Yan, Bryan P.: The Chinese University of Hong Kong, Hong Kong
Yasuda, Satoshi: Tohoku University Graduate School of Medicine, Sendai, Japan
Ye, Jong Chul: Korea Advanced Institute of Science and Technology, Daejeon, South Korea
Yu, Bo: The Second Affiliated Hospital of Harbin Medical University, Harbin, China

[5]Hospital Clínico San Carlos Madrid Spain

[6]German Heart Center, Munich, Germany

[7]University Hospitals Bristol and Weston NHS Foundation Trust, Bristol, United Kingdom

[8]Inselspital, Bern University Hospital, University of Bern, Bern, Switzerland

[9]University Hospitals Leuven, Leuven, Belgium

[10]UniCamillus - Saint Camillus International University of Health Sciences, Rome, Italy

[11]University of Giessen, Giessen, Germany

[12]University of Vermont, Burlington, Vermont, USA

[13]University of Texas Health, San Antonio, Texas, USA

[14]Icahn School of Medicine at Mount Sinai, New York, New York, USA

[15]New York Presbyterian Hospital, Columbia University Medical Center and Cardiovascular Research Foundation, New York, New York, USA

[16]MedStar Washington Hospital Center, Washington, DC, USA

[17]Cardiovascular Research Foundation, New York, New York, USA

[18]Institut Mutualiste Montsouris, Paris, France

[19]University Hospital of Clermont Ferrand, Clermont-Ferrand, France

[20]University Hospital Jean Minjoz, Besançon, France

[21]Aarhus University Hospital, Skejby, Denmark

[22]Hospital Universitario La Princesa, Madrid, Spain

[23]Hospital Clinico San Carlos, IdISSC, Universidad Complutense, Madrid, Spain

[24]Fondazione Policlinico Universitario A. Gemelli IRCCS, Università Cattolica del Sacro Cuore, Rome, Italy

[25]Yonsei University College of Medicine, Seoul, South Korea

[26]The Prince Charles Hospital, Chermside, Queensland, Australia

[27]University of Melbourne, Melbourne, Victoria, Australia

[28]Barts Health NHS Trust, London, United Kingdom, University College London, London, United Kingdom, and Queen Mary University London, London, United Kingdom

[29]Tokyo Medical and Dental University, Tokyo, Japan

[30]Kitasato University School of Medicine, Kanagawa, Japan

[31]Showa University Hospital, Tokyo, Japan

[32]Kawasaki Medical School, Okayama, Japan

[33]Tsuchiura Kyodo General Hospital, Ibaraki, Japan

[34]Massachusetts Institute of Technology, Cambridge, Massachusetts, USA

Abstract

Since optical coherence tomography (OCT) was first performed in humans two decades ago, this imaging modality has been widely adopted in research on coronary atherosclerosis and adopted clinically for the optimization of percutaneous coronary intervention. In the past 10 years, substantial advances have been made in the understanding of in vivo vascular biology using OCT. Identification by OCT of culprit plaque pathology could potentially lead to a major shift in the management of patients with acute coronary syndromes. Detection by OCT of healed coronary plaque has been important in our understanding of the mechanisms involved in plaque destabilization and healing with the rapid progression of atherosclerosis. Accurate detection by OCT of sequelae from percutaneous coronary interventions that might be missed by angiography could improve clinical outcomes. In addition, OCT has become an essential diagnostic modality for myocardial infarction with non-obstructive coronary arteries. Insight into neoatherosclerosis from OCT could improve our understanding of the mechanisms of very late stent thrombosis.

The appropriate use of OCT depends on accurate interpretation and understanding of the clinical significance of OCT findings. In this Review, we summarize the state of the art in cardiac OCT and facilitate the uniform use of this modality in coronary atherosclerosis. Contributions have been made by clinicians and investigators worldwide with extensive experience in OCT, with the aim that this document will serve as a standard reference for future research and clinical application.

Graphical Abstract

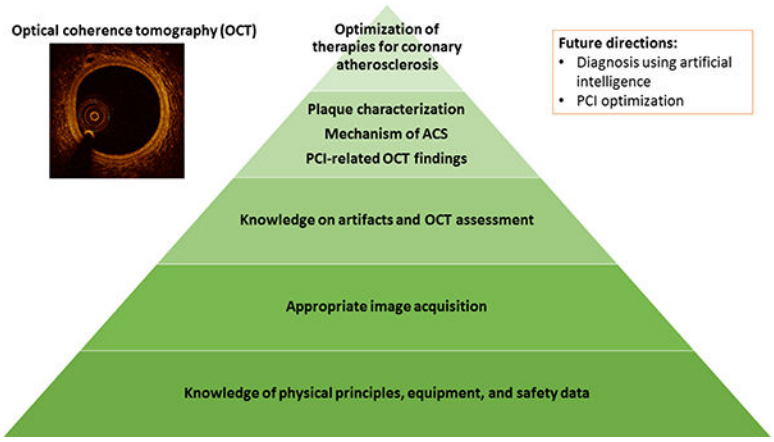

Appropriate use of optical coherence tomography (OCT) for optimization of therapies for coronary atherosclerosis is based on proper knowledge of the methodology, terminology, and clinical relevance of OCT. Global input from clinicians and investigators with extensive OCT experience from the United States, Asia, Canada, India, and Australia was incorporated, with the aim of promoting the uniform use of OCT in coronary atherosclerosis. ACS = acute coronary syndrome

Keywords

optical coherence tomography; expert review; atherosclerosis; coronary artery disease; percutaneous coronary intervention; stent

Introduction

Optical coherence tomography (OCT) is an imaging technology for evaluating the microstructure of coronary arteries at an axial resolution of approximately 10–15 μm.[1] Due to its higher axial resolution than intravascular ultrasound (IVUS), OCT can characterize the superficial structure of the vessel wall in greater detail.[2–4] Over the past two decades, a large number of OCT studies have been reported.

The utility of OCT imaging is based on correct acquisition and interpretation of images as well as knowledge of the currently available evidence. This document aims to facilitate the uniform use of OCT in coronary atherosclerosis. Global input from clinicians and investigators with extensive OCT experience was incorporated into the original draft prepared at the Massachusetts General Hospital (MGH) on the methodology, terminology, and clinical relevance of OCT. More than one hundred OCT experts from Europe, the United States, Asia, Canada, India, and Australia endorsed this review document (listed at the end of the text). The strategy for intracoronary imaging-guided optimization of percutaneous coronary intervention (PCI) largely followed the recommendations of the European Association of PCI (EAPCI).[5, 6]

At present, there are two major commercially available intracoronary optical-based imaging systems: OCT made by Abbott Vascular (Santa Clara, CA, USA) and optical frequency domain imaging (OFDI) made by Terumo Corporation (Tokyo, Japan). Since there is no difference in the image interpretation between the two systems, the following descriptions about OCT also apply to OFDI.

Physical principles of OCT imaging

OCT is a near-infrared, light-based imaging modality that generates high-resolution cross-sectional images of tissue microstructure.[1] The penetration depth depends on the tissue type and ranges from 0.1 to 2.0 mm, which is less than IVUS. Physical principles of OCT imaging are detailed in the Supplementary Material. OCT equipment is also described in the Supplementary Material.

OCT image acquisition

OCT should be used with caution in patients with a single remaining vessel, markedly impaired renal function, or known allergy to contrast media. In lesions with near-complete or total occlusion of the artery, it is recommended that antegrade blood flow is restored before OCT examination to allow the flushing media to adequately clear blood from the artery. This can usually be achieved by pre-dilatation using an under-sized balloon or by aspiration thrombectomy. If subintimal wiring is suspected in cases of chronic total occlusion, OCT should be spared because injection of flushing media may force progression of coronary dissections. OCT catheters are sometimes unable to pass through severely narrowed, calcified, or tortuous lesions or may be unable to follow the guide wire in arteries such as the left circumflex with a sharp angle from the left main coronary artery. The use of a guide extension catheter may help to deliver the catheter into the left circumflex without prolapse.

If not contraindicated, image acquisition should be conducted after the administration of intracoronary nitroglycerin to minimize catheter-induced vasospasm with appropriate attention to anticoagulation. OCT imaging catheters require careful purging with viscous undiluted contrast to remove air or blood before the interrogation. The OCT imaging catheter is advanced into the distal coronary artery over a standard angioplasty guide wire (0.014-inch). Automated OCT pullback is performed during either manual contrast injection through the guiding catheter using a syringe or automatically using a power injector (typical flush rate 4.0–5.5 ml/s for the left coronary artery and 3.0–4.0 ml/s for the right coronary artery at 300–400 psi).

Coaxial positioning of the guiding catheter into the coronary ostium is important for obtaining optimal blood clearance. A 6-Fr or larger diameter guiding catheter is recommended but OCT imaging catheters also fit 5-Fr guiding catheters or 6-Fr guide extensions. A guiding catheter without side holes may facilitate blood clearance. OCT acquisition can be performed through guide extension catheters. This approach may allow better target vessel intubation, providing high quality images for coronary ostial lesions and reducing contrast volume.

Since higher viscosity solutions provide superior results, iso-osmolar contrast media is used for flushing. In patients with impaired renal function, low molecular weight dextran, normal saline, or diluted contrast media may substitute for contrast media. It should be noted that low molecular weight dextran also has renal toxicity.

Understanding potential complications related to OCT imaging is important. In a prospective registry, catheter-related complications occurred in 0.6% and they were either self-limiting after retrieval of the imaging catheter or easily treatable in the catheterization laboratory.[7] Contrast injection should be terminated as soon as imaging of the target segment has been completed because contrast volume during pullback was reported to be a risk factor for malignant arrhythmias.[8] Safety data are detailed in the Supplementary Material.

OCT image display

There are three modes for displaying OCT images: the traditional cross-sectional image (orthogonal to the vessel), longitudinal view, and 3-dimensional visualization. These are detailed in the Supplementary Material. Contemporary OCT systems provide co-registration with angiography to allow matching cross-sectional OCT images with their position on angiograms, which facilitates plaque assessment and optimization of PCI.

OCT artifacts

The recognition of artifacts is critical for the correct interpretation of images. The OCT artifacts are summarized in Table 1 and representative images are shown in Figure 1.

Basic measurements

It has been reported that reproducibility of OCT measurements was high.[10–14] Meaningful measurements require good-quality images that contain no or minimal artifacts. Although OCT systems provide automatic lumen detection, manual correction is required especially

when the image quality is suboptimal. To make accurate measurements, the image should be correctly calibrated for z-offset. Although OCT systems offer an automated calibration, manual correction is sometimes required. Since calibration can vary depending on flushing medium, this needs to be adjusted. Proximal or distal reference is defined as the site with the largest lumen proximal or distal to a stenosis but within the same segment (usually within 10 mm of the stenosis, with no major intervening branches).[9] This may not be the site with the least plaque.

The definition of measurements are as follows:

Arc. Arc measured using the center of the lumen as the vertex.

Depth. The distance between the luminal border and the adluminal surface of the plaque feature.

Thickness. The thickest distance between the inner and outer border of the plaque component (valid only if the deep boundary can be identified).

Area. The cross-sectional area (CSA) of the plaque component (valid only if the deep boundary can be identified).

Volume. The sum of areas of each cross-section multiplied by the slice thickness over the segment of interest (Simpson's rule).

Cap thickness. The thickness of a cap present over calcium or lipid. Minimum fibrous cap thickness is conventionally measured 3 times at the thinnest point in magnified views, and the average value is calculated.[15]

Lesion length. The distance between the proximal and distal reference. Length measurement is detailed in the Supplementary Material.

Vessel and plaque morphology

Since OCT acquires multiple sequential images during the pullback, confirming a finding in more than one frame helps to improve diagnostic confidence. The following image interpretations are widely accepted.

Normal vessel wall—The media of the normal vessel appears as a lower signal intensity band relative to that of the intima and adventitia, providing a three-layered appearance (bright-dark-bright) (Figure 2A). The internal elastic membrane (IEM), or internal elastic lamina is defined as the border between the intima and media. The external elastic membrane (EEM), or external elastic lamina is defined as the border between the media and the adventitia. These membranes may be visualized as highly backscattering thin structures. Intimal thickening occurs during the early phase of coronary atherosclerosis[16] and is represented as a signal-rich homogeneous thick intimal band in OCT images (Figure 2B). The definition of intimal thickening is limited by the lack of an established cutoff value.

Atherosclerotic plaque—An atherosclerotic plaque is defined as a mass lesion (focal thickening) or loss of a layered structure of the vessel wall.

Fibrous plaque—Fibrous plaque exhibits homogeneous, signal-rich (highly backscattering) regions (Figure 2C). Sometimes, the limited penetration depth of OCT precludes the accurate detection of signal-poor regions located deep within the vessel wall thereby limiting the assessment of lipid or calcium behind fibrous tissue.

Calcified plaque—Calcified plaque exhibits signal-poor regions with sharply delineated borders and limited shadowing (Figure 2D). Unlike IVUS, OCT can finely delineate calcification as OCT light penetrates calcium and it permits the quantification of both the arc and thickness[17] if calcium is not too thick[18]. Calcification thickness can be measured only when both leading and trailing edges are visible. Calcium length is measured on the longitudinal view. Calcium index is calculated as the product of calcium arc and calcium length. These measurements can have a bearing on how to best prepare a calcified lesion before stent implantation. The EAPCI document recognized that a calcium arc >180° and calcium thickness >0.5 mm are risk factors for stent underexpansion.[5]

Lipid plaque—Lipid plaque exhibits signal-poor regions with diffuse borders (lipid pool) and overlying signal-rich bands (fibrous caps), accompanied by high signal attenuation (Figure 2E). Histopathologic validation studies show a good correlation between signal-poor OCT regions with diffuse borders and lipid pools on histology, corresponding to either a necrotic core or a region within pathological intimal thickening that contains extracellular lipid and/or proteoglycans.[4, 19, 20]

Due to the limited penetration depth of OCT for lipid-containing tissues, OCT is not capable of measuring the thickness, area, or volume of lipids. Instead, the circumferential arc is used to semi-quantify lipids. Lipid-rich plaque is defined as a lipid plaque that has a lipid arc of >90°.[21] Lipid length is measured on the longitudinal view. Lipid index is calculated as the product of mean lipid arc and lipid length.[22]

Thin-cap fibroatheroma (TCFA)—TCFA is defined as a lipid plaque in which the minimum thickness of the fibrous cap is less than a predetermined threshold and lipid occupies >90° in circumference (Figure 2F). The most frequently adopted cutoff minimal cap thickness is 65 μm, derived from histology studies.[23] However, caution should be taken when a cutoff is directly applied to OCT because tissue shrinkage can occur during histopathologic tissue processing and only fatal cases were assessed. Thus, the true minimal fibrous cap thickness that may predispose to plaque rupture may be >65 μm, although it is presently uncertain. A cutoff thickness of 80 μm is sometimes used.[24] Semi-automated assessment of cap thickness[25] and 3-dimensional measurement of the surface area of the thin fibrous cap[26] have been reported. It should be noted that tangential signal dropout may falsely create the appearance of a TCFA (Table 1) (Figure 1G).

Macrophages—Macrophages are inflammatory cells located in the fibrous tissue covering a lipid plaque and occasionally in fibrous plaque. Macrophages appear in OCT as signal-rich, distinct, or confluent punctate regions that exceed the intensity of background

speckle noise[27] (Figure 3A). Due to their high backscatter and attenuation characteristics, macrophages cast a dark shadow behind their aggregates. Macrophages frequently cluster together, forming a band of highly reflective tissue, which causes a plaque to appear as if it is a TCFA (Supplementary Figure 1). The strong attenuating properties of macrophage aggregates cause the casting of a laterally sharp shadow and rapid change in appearance from frame to frame. This typical characteristic helps to differentiate a band of macrophages overlying a fibroatheroma from a true TCFA. A detailed classification of macrophages into lines or dots has been reported.[28] Quantification of macrophages has been attempted using a parameter termed the normalized standard deviation.[27, 29] Semi-quantification (grade 0–4) has also been reported.[30, 31] It is important to note that rigorous histology validation of macrophage on OCT has not been yet reported.

Microvessels—With the gradually increasing size of the plaque, nurturing vessels, known as microvessels (or microchannels) can be observed. Microvessels promote the influx of lipid materials, and the infiltration of inflammatory or red blood cells within coronary plaques.[32] Microvessels within the intima can appear in OCT as signal-poor voids that are sharply delineated and can usually be followed in multiple contiguous frames (Figure 3B).[33] A cutoff value of 50–300 μm in diameter and a requirement of the extension in at least 3 consecutive frames are sometimes adopted to define microvessels.[33] As these microvessels communicate with the periadventitial vasculature and eventually with the lumen of the coronary artery, their blood content is flushed during an OCT pullback. To discriminate larger microvessels from small side branches, an inspection of adjacent frames is helpful. The accuracy of microvessel detection decreases in lipid plaques in which the penetration of OCT light is hampered. It has not been fully clarified if these microvessels communicate with the luminal surface or emanate from the vasa vasorum. Detection and quantification of adventitial vasa vasorum have been attempted.[34, 35] Further studies are required to explore this issue.

Cholesterol crystals—Cholesterol expands in volume when crystallizing from a liquid to a solid state and may cause plaque volume expansion.[36, 37] Both *ex vivo* human studies, as well as animal studies, suggest that sharp-tipped cholesterol crystals may perforate the fibrous cap.[38] Cholesterol crystals appear in OCT as thin, linear regions of high intensity, usually in proximity of a lipid plaque (Figure 3C). In one histology study, the sensitivity of OCT for detecting cholesterol crystals was only 68%.[39] In another histology study, the sensitivity of OCT for detecting cholesterol crystals was 26% even after a modification to the definition of cholesterol crystals.[40] It should be noted that some cholesterol crystals visualized in histology are not visualized by OCT, particularly when cholesterol crystals are aligned tangential to the OCT light beam.

Thrombus—Destabilization of plaque leading to subsequent thrombotic occlusion of the coronary artery accounts for the majority of acute coronary events. Thrombus by OCT appears as a protruding mass attached to the luminal surface or floating within the lumen. OCT can discriminate between 2 types of thrombus: red (erythrocyte-rich) thrombus (Figure 3D), which is highly backscattering and has a high attenuation (resembles blood), and white (platelet-rich) thrombus (Figure 3E), which is less backscattering, is

homogeneous, and has lower attenuation. Since red blood cells reflect light, red thrombus typically shadows or obscures underlying structures, while platelet thrombus does not. Spontaneous recanalized coronary thrombus may appear as signal-rich, high backscattered septa dividing the lumen into multiple small cavities with smooth inner borders, which is known as “honeycomb” appearance.[41, 42] However, this finding requires further histological validation. The thrombus score is calculated by summing the number of involved quadrants (0, 1, 2, 3, or 4) in each cross-sectional image through the longitudinal length of the thrombus.[43] The thrombus area is measured by tracing outlines of the thrombus on cross-sectional images. The thrombus volume is calculated by mean thrombus area multiplied by thrombus length.[44, 45]

Layered plaque—Pathology studies have shown that atherosclerotic plaques might destabilize without clinical consequences.[46, 47] Whether an acute coronary syndrome (ACS) develops following disruption of a plaque depends on the severity of stenosis and the balance between systemic/local thrombogenicity and endogenous anti-thrombotic/thrombolysis mechanisms. Thrombus becomes organized, with connective tissue deposition of predominantly proteoglycans and type III collagen.[48, 49] During the healing process, type III collagen is gradually replaced by type I collagen, which appears as a band of high backscattering signal on OCT.[48, 49] A histological validation study reported excellent agreement between healed plaques on pathology and layered plaques on OCT.[50] Layered plaque is defined as plaque with one or more layers of different optical densities and a clear demarcation from underlying components (Figure 3F).[48] Serial OCT assessments in large and well-characterized study populations are required to better understand this process.

Intraplaque hemorrhage—OCT has never been validated for the diagnosis of intraplaque hemorrhage. Only two case reports have been published so far, in which OCT images showed a clearly bordered, crescent-shaped low-signal region.[51, 52] Histological validation studies are required for this finding.

Other lesion morphologies—Aneurysms and transplant vasculopathy are described in the Supplementary Material.

Lumen measurements

Lumen area. The area bounded by the luminal border.

Minimum lumen diameter. The shortest diameter through the center of mass of the lumen.

Maximum lumen diameter. The longest diameter through the center of mass of the lumen.

Lumen eccentricity. (Maximum lumen diameter minus minimum lumen diameter) divided by maximum lumen diameter.

Minimum lumen area (MLA). The smallest lumen area along the length of the target lesion.

Percent area stenosis (%AS). (Reference lumen area minus MLA) divided by reference lumen area multiplied by 100. The reference segment used should be specified (proximal, distal, largest, or average).

IEM measurements

For plaques in which the IEM can be identified, area and diameter can be measured for the IEM. In the presence of a large plaque burden or lipid, OCT fails to visualize the entire circumference of the IEM. Consequently, IEM measurements can be made only for those plaques in which the IEM can be identified for ≥180 degrees. IEM measurements are detailed in the Supplementary Material. These can also be applied for the EEM measurements. Attenuation compensation technique, a post-processing methodology to enhance the EEM has been reported.[53, 54]

OCT for mechanisms of ACS

OCT can accurately assess vessel and lumen geometry and identify the hallmark of a culprit lesion including plaque disruption and thrombus.[55] A better understanding of mechanisms of ACS has a significant impact on patient management.

Plaque rupture—Plaque rupture occurs in the context of TCFAs and shows a disruption of the fibrous cap[56] (Figure 4A). When injected with optically transparent contrast media, the disruption may appear as a hollow cavity. Thrombi are often found overlying the ruptured cap. However, thrombus may be absent at the site of an old plaque rupture or with acute rupture treated with anti-thrombotic or thrombolytic therapies. It should be noted that the presence of a large luminal red thrombus obscures the underlying component, rendering the reliable diagnosis of plaque rupture difficult. Assessing contiguous frames rather than a single frame helps to differentiate plaque rupture from other components such as side branches and artifacts.

Plaque erosion—The pathology definition of plaque erosion is endothelial denudation with thrombosis without evidence of plaque rupture.[56] As the detection of an endothelial monolayer (i.e., 1–5 μm) is below the resolution of the current OCT systems, plaque erosion remains a diagnosis of exclusion *in vivo*. In the criteria developed for the diagnosis of plaque erosion by OCT,[57] definite erosion was defined as the presence of attached thrombus overlying an intact and visualized plaque (Figure 4B). Probable erosion was defined by luminal surface irregularity at the culprit lesion in the absence of thrombus (Figure 4C) or attenuation of underlying plaque by thrombus without superficial lipid or calcification immediately proximal or distal to the site of thrombus. An algorithm for the diagnosis of plaque erosion is presented in Supplementary Figure 2. As these criteria lack the precision of the pathology definition of erosion, some studies call this entity an intact fibrous cap.[58] Plaque erosion is predominantly accompanied by white thrombus rather than red thrombus. When a large red thrombus is present, which attenuates the OCT light, the diagnosis of plaque erosion becomes less definite as plaque rupture cannot be excluded. Identification of plaque erosion may facilitate tailoring of patient treatment. Proof-of-concept studies have demonstrated that plaque erosion associated with a residual diameter stenosis <70% may be treated with anti-thrombotic therapy without stenting.[59–62] Larger randomized controlled studies are needed to further explore this concept.

Eruptive calcified nodule—Eruptive calcified nodule is characterized by an underlying heavily calcified plaque with a distinct nodular mass of calcium that protrudes into the

lumen and causes dysfunction or loss of the overlying endothelial cells.[63] Eruptive calcified nodules appear in OCT as single or multiple regions of calcium that protrude into the lumen with fibrous cap disruption, frequently forming sharp, protruding edges, and the presence of substantive calcium proximal and/or distal to the lesion[18] (Figure 4D). It should be noted that the attenuation of OCT light from protruding calcium conceals deeper structures, rendering the differentiation from red thrombus difficult. Eruptive calcified nodule is typically found in elderly or dialysis patients with heavily calcified vessels at hinge points. Eruptive calcified nodule is associated with a higher rate of target vessel failure after PCI, highlighting the complex nature of this lesion.[64, 65] *In vivo* classification of calcific plaque-related ACS has been proposed, which included eruptive calcified nodule, superficial calcific sheet (Supplementary Figure 3A), and calcified protrusion (Supplementary Figure 3B).[66] In this study, superficial calcific sheet, which was frequently located in the left anterior descending artery, was the most prevalent type and associated with greatest post-PCI myocardial damage. However, this classification lacked histological validations.

Spontaneous coronary artery dissection (SCAD)—SCAD is observed in 2–4% of angiograms performed for ACS[67, 68] and is more frequent in young to middle-aged women[69]. The hallmark appearance in OCT is an accumulation of blood or flushing media within the medial space, displacing the IEM inward and EEM outward (intramural hematoma), with or without communication with the lumen (intimal tear) (Figure 4E). It is rare to observe overlying thrombus in SCAD. OCT may provide greater diagnostic clarity than IVUS in assessing the distinctive features of intramural hematoma and/or intimal tear. However, the instrumentation and injection of contrast media into a dissected vessel carries the risk of propagation of dissection and vessel closure. Therefore, OCT imaging should be reserved for cases where diagnostic uncertainty persists, particularly angiographic SCAD type 3 and 4.[70]

Myocardial infarction with nonobstructive coronary arteries (MINOCA)—MINOCA accounts for 6–15% of cases of spontaneous MI and frequently affects females.[71] Pathogenesis of MINOCA is varied and may include vascular etiologies such as plaque rupture, erosion, vasospasm, embolization, SCAD, or microvascular disease, of which findings are often angiographically inapparent. Incomplete understanding of mechanisms of ACS leads to variable use of diagnostic testing and medical therapies for secondary prevention with potentially higher costs and lesser efficacy. In the absence of significant obstructive lesions on angiography, the physician should consider non-atherosclerotic etiologies, particularly if patients present with atypical symptoms or unusual demographic/clinical risk profiles. OCT is an invaluable tool to detect atherosclerotic plaque disruption or non-atherosclerotic arterial pathology.[72–74]

OCT for detection of vulnerable plaque

Detection of vulnerable plaque has been one of the main focuses of OCT research. There is ongoing controversy on detection of vulnerable plaque and preemptive local treatment.[75] Clinical outcomes of preemptive stenting are being investigated in the PREVENT study, in which patients with high-risk features identified by IVUS, near-infrared spectroscopy (NIRS), or OCT are randomized to PCI plus medication vs. medication alone

(NCT02316886). Detection of vulnerable plaque may help to identify patients who benefit from aggressive prevention treatments such as PCSK9 inhibitors or anti-inflammatory therapies. This topic is detailed in the Supplementary Material.

PCI-related OCT findings

Basic stent measurements—Descriptions are provided in the Supplementary Material.

Stent underexpansion—Stent expansion describes the minimum stent area (MSA) either as an absolute expansion (MSA itself) or relative expansion (MSA divided by the mean of the proximal and distal reference lumen areas). Small MSA is known as a predictor of suboptimal post-PCI fractional flow reserve (FFR)[76] and adverse outcomes[77, 78]. Different targets of stent expansion have been adopted in clinical trials that assessed the impact of OCT-guided PCI.[79–82] The EAPCI document recommended a relative expansion >80% as a goal of optimization.[5] It should be noted that a relative expansion >80% may result in a small MSA in small vessels. There is ongoing controversies on this recommendation.

Malapposition—OCT enables accurate assessment of apposition of stent struts to the arterial wall. If the axial distance between the strut's surface to the luminal surface is greater than the strut thickness (including polymer, if present), the strut is considered malapposed (Figure 5A). Differences in strut thickness across different stents should be taken into consideration. OCT studies have reported that malapposition was associated with acute (<1 day), subacute (1–30 days), late (30 days–1 year), and very late (>1 year) stent thrombosis.[83, 84] However, malapposition noted at the time of stent thrombosis may either have been present after the index PCI (persistent malapposition) or developed during follow-up (late-acquired malapposition) due to thrombus resolution or vascular toxicity from the stent. Further studies are required to determine if malapposition is an independent risk factor for stent thrombosis. Malapposition increases the risk of accidental abluminal rewiring and deformation of stent in aorto-ostial segment due to collision with the guiding catheter. The EAPCI document[5] recommended not correcting acute malapposition of <0.4 mm with longitudinal extension <1 mm as spontaneous neointimal integration is anticipated.

Tissue prolapse—Tissue prolapse between stent struts toward the lumen may represent protrusion of non-calcified plaque or, in the context of ACS, of atherothrombotic material (Figure 5B). OCT enables clearer visualization of tissue prolapse than IVUS. Tissue prolapse is more frequently observed when the stent is placed over a lipid-rich plaque or TCFA. In patients with ACS, tissue prolapse has been reported to be a predictor of target lesion revascularization.[78, 85] There is insufficient evidence to act with further intervention on tissue prolapse.

Dissection—OCT allows visualization of subtle stent edge dissections typically missed by IVUS (Figure 5C). ILUMIEN III classified edge dissections as major, when dissection extends ≥60° of the circumference of the vessel or ≥3 mm in length.[81] In the CLI-OPCI II study[77], distal edge dissection with a width ≥200 μm was a predictor of adverse events. In contrast, in a multicenter OCT registry, stent edge dissections were not associated with adverse events.[78] Minor edge dissections are unlikely to be clinically relevant.[86, 87]

Dissections can lead to intramural hematoma that sometimes progresses and may result in acute vessel closure, particularly when the hematoma is at the distal stent edge. The EAPCI document recognized the presence of residual plaque burden, extensive lateral (>60°), and longitudinal extension (>2 mm), involvement of deeper layers (medial or adventitia) and localization distal to the stent increase the risk for adverse events.[5]

OCT for optimization of PCI

OCT provides information that can be used to optimize stent implantation and minimize stent-related complications. The size and length of balloon and stent are decided based on the pre-PCI OCT measurements, which are more accurate than those obtained by quantitative coronary angiography. Plaque morphology should be assessed before treatment to guide lesion preparation and stent selection. For a heavily calcified lesion, a debulking technique such as atherectomy or intravascular lithotripsy (IVL) may be considered for better lesion preparation to avoid underexpansion. OCT is valuable to confirm calcium fracture, which is associated with better stent expansion[88]. Where pre-dilatation or debulking technique was performed, OCT imaging should be repeated to confirm sufficient lesion preparation and optimize the stent sizing.

The normal, or near normal segment in the case of a diffusely diseased artery, that is the closest to the target lesion can be used as a landing zone of the stent. Since the presence of lipid-rich plaque at the landing zone is associated with a higher risk of periprocedural MI[89] and stent edge restenosis[90], landing in a lipid-rich area should be avoided. The EAPCI document proposed the use of the mean distal lumen diameter with up rounding the stent diameter (e.g. 3.76→4.0 mm) or the mean EEM (2 orthogonal measurements) with down rounding the stent diameter (e.g. 3.76→3.5 mm).[5] Practical strategies of OCT-based optimization of PCI are detailed in the EAPCI document.[5] Additional details of OCT-guided PCI are summarized in the Supplementary Material.

OCT-guided PCI vs. physiological indices-guided PCI—PCI for stable angina is indicated for hemodynamically significant coronary stenoses.[91, 92] Pressure-derived invasive indices have been accepted as the gold standard for invasive ischemia assessment.[91, 93] A randomized trial that included angiographically intermediate stenosis demonstrated a lower occurrence of adverse events in OCT-guided PCI than in FFR-guided PCI.[94] The impact of the addition of OCT to FFR on clinical outcomes is being investigated in a randomized trial (NCT02989740).[95] Several studies have reported that lumen measurements and plaque morphology assessed by OCT correlate with FFR.[96–98] A slight superiority of OCT over IVUS for the detection of FFR-positive lesions has been reported.[99, 100] Optical flow ratio (OFR) is an OCT-based method for functional assessment of coronary stenosis based on computational fluid dynamics. OFR showed an excellent agreement with FFR and was superior to MLA in the detection of physiologically significant stenosis.[101, 102] Post-PCI OFR showed good diagnostic concordance with post-PCI FFR.[103] Further studies are warranted on this topic.

OCT for bifurcation lesions—OCT provides useful guidance in the treatment of bifurcation lesions.[104] OCT depicts an ostial lesion in bifurcation without overlap and

foreshortening, which frequently occur on angiograms. Three-dimensional reconstruction can be used to understand the geometry and morphology of bifurcation lesions. Following stent implantation, OCT can guide the re-crossing of guide wires through stent struts jailing the side branch ostium (Supplementary Figure 4), and confirm optimization of bifurcation segments, the clinical significance of which is being tested in the OCTOBER study (NCT03171311).[105] A randomized trial demonstrated that three-dimensional-OFDI-guidance was superior to angiography-guidance in terms of acute stent apposition at bifurcation.[106] The LEMON study reported the feasibility and performance of OCT-guided left main stem PCI according to a pre-specified protocol, in which OCT guidance modified operators' strategy in 26% of the patients.[107] The use of OCT in bifurcation lesions is detailed in the document from European and Japanese bifurcation clubs.[108]

Late stent change

Strut coverage—The low susceptibility of OCT to artifacts at the stent strut enables the visualization of tissue overlying struts and the evaluation of the response to stent implantation. Struts are termed "covered" if any tissue can be identified above the struts (Figure 6A) and "uncovered" if no evidence of tissue can be visualized above the struts (Figure 6B). The coverage thickness can be measured as the distance between the adluminal surface of the covered tissue and abluminal reflective edge of metallic struts. Whether the tissue is fibrin, endothelium, thrombus, mature neointima, or other cannot be ascertained at present because a single cell endothelial layer is beyond the limits of resolution of OCT and the nature of tissue cannot be differentiated. Tissue characteristics such as backscattering intensity may provide further discrimination of tissue type.[109] A threshold of tissue above struts ≥40 μm was reported to help to detect healthy strut coverage.[110] However, this issue needs further investigation. In addition, whether the tissue is non- or less-thrombogenic is unknown. As with apposition, strut coverage can be reported per strut, per cross-section, or per stent. Percentage of uncovered struts can be measured as the number of struts without distinct overlying tissue, in which the luminal reflection of the strut surface is directly interfacing with the lumen, divided by a total number of analyzable struts × 100.

Evagination—Stent implantation, and the ensuing mechanical trauma and inflammatory reactions, may lead to vascular positive remodeling, causing evagination. Evagination appears in OCT as an outward bulge in the luminal vessel contour between apposed struts (Figure 6C). In a retrospective study, evagination was more frequent in first-generation drug-eluting stents (DES).[111] Further studies are needed to better understand this finding.

Classification of neointima—OCT provides detailed morphological information about neointimal tissue within stents. Neointimal tissue has been historically subdivided into three different patterns by OCT: 1) homogeneous, 2) heterogeneous, and 3) layered, each of which is detailed in the Supplementary Material. Neointimal patterns might offer guidance to the treatment of in-stent restenosis.[112] However, this issue needs further investigation.

Neoatherosclerosis—Clinical trials have shown continuous target lesion revascularization over time, irrespective of the generation of the stent.[113] Atherosclerotic changes within the neointima play an important role in the development of stent-related

adverse events. Neoatherosclerosis is defined by the presence of at least one of the components of a mature atherosclerotic plaque such as lipid-laden tissue or calcification within the stent (Figure 6D). Neoatherosclerosis increases with time after stenting and appears in an earlier phase in DES than in bare-metal stent.[114–116] Neoatherosclerosis and subsequent disruption of lipid-laden neointima have been known to be associated with very late stent thrombosis.[83, 117–119]

Serial OCT examination

Longitudinal studies (baseline versus follow-up) can be used to evaluate the progression or regression of coronary atherosclerosis and the response to stent implantation. This topic is described in the Supplementary Material.

Future directions

Under-utilization of OCT is persisting in most regions of the world due to hurdles such as increased procedure time, lack of reimbursement, and the need for education. Artificial intelligence may aid physicians with tissue characterization and guidance in stent sizing and optimization.[121, 122]

Hybrid OCT-based imaging such as IVUS-OCT[123], OCT-NIRS[124], OCT-near-infrared fluorescence[125], and OCT-fluorescence lifetime imaging microscopy[126], higher resolution OCT (micro-OCT)[127], and polarization-sensitive OCT[128] are also being developed and may provide additional insights in the assessment of coronary atherosclerosis.

Conclusions

The past two decades have witnessed the generation of an enormous amount of data from cardiac OCT research. OCT has helped us to better understand the underlying mechanisms of ACS. Detection of plaque erosion in patients with ACS is one of the major advances in the study of *in vivo* vascular biology in recent years. Layered (healed) coronary plaque research provided insights into the mechanisms of plaque destabilization and healing. Detailed information obtained by OCT during PCI may potentially improve clinical outcomes. Further studies are needed to establish a clear role for OCT in cardiology.

Supplementary Material

Refer to Web version on PubMed Central for supplementary material.

Acknowledgments

We would like to thank all the investigators around the globe for their contributions.

References

1. Huang D, Swanson EA, Lin CP, Schuman JS, Stinson WG, Chang W, Hee MR, Flotte T, Gregory K, Puliafito CA, et al. Optical coherence tomography. Science 1991;254(5035):1178–81. [PubMed: 1957169]

2. Brezinski ME, Tearney GJ, Bouma BE, Izatt JA, Hee MR, Swanson EA, Southern JF, Fujimoto JG. Optical coherence tomography for optical biopsy. Properties and demonstration of vascular pathology. Circulation 1996;93(6):1206–13. [PubMed: 8653843]

3. Jang IK, Bouma BE, Kang DH, Park SJ, Park SW, Seung KB, Choi KB, Shishkov M, Schlendorf K, Pomerantsev E, Houser SL, Aretz HT, Tearney GJ. Visualization of coronary atherosclerotic plaques in patients using optical coherence tomography: comparison with intravascular ultrasound. J Am Coll Cardiol 2002;39(4):604–9. [PubMed: 11849858]

4. Yabushita H, Bouma BE, Houser SL, Aretz HT, Jang I-K, Schlendorf KH, Kauffman CR, Shishkov M, Kang D-H, Halpern EF, Tearney GJ. Characterization of Human Atherosclerosis by Optical Coherence Tomography. Circulation 2002;106(13):1640–1645. [PubMed: 12270856]

5. Raber L, Mintz GS, Koskinas KC, Johnson TW, Holm NR, Onuma Y, Radu MD, Joner M, Yu B, Jia H, Meneveau N, de la Torre Hernandez JM, Escaned J, Hill J, Prati F, Colombo A, di Mario C, Regar E, Capodanno D, Wijns W, Byrne RA, Guagliumi G, Group ESCSD. Clinical use of intracoronary imaging. Part 1: guidance and optimization of coronary interventions. An expert consensus document of the European Association of Percutaneous Cardiovascular Interventions. Eur Heart J 2018;39(35):3281–3300. [PubMed: 29790954]

6. Johnson TW, Raber L, di Mario C, Bourantas C, Jia H, Mattesini A, Gonzalo N, de la Torre Hernandez JM, Prati F, Koskinas K, Joner M, Radu MD, Erlinge D, Regar E, Kunadian V, Maehara A, Byrne RA, Capodanno D, Akasaka T, Wijns W, Mintz GS, Guagliumi G. Clinical use of intracoronary imaging. Part 2: acute coronary syndromes, ambiguous coronary angiography findings, and guiding interventional decision-making: an expert consensus document of the European Association of Percutaneous Cardiovascular Interventions. Eur Heart J 2019;40(31):2566–2584. [PubMed: 31112213]

7. van der Sijde JN, Karanasos A, van Ditzhuijzen NS, Okamura T, van Geuns RJ, Valgimigli M, Ligthart JM, Witberg KT, Wemelsfelder S, Fam JM, Zhang B, Diletti R, de Jaegere PP, van Mieghem NM, van Soest G, Zijlstra F, van Domburg RT, Regar E. Safety of optical coherence tomography in daily practice: a comparison with intravascular ultrasound. Eur Heart J Cardiovasc Imaging 2017;18(4):467–474. [PubMed: 26992420]

8. Terada N, Kuramochi T, Sugiyama T, Kanaji Y, Hoshino M, Usui E, Yamaguchi M, Hada M, Misawa T, Sumino Y, Hirano H, Nogami K, Ueno H, Wakasa N, Hosokawa M, Murai T, Lee T, Yonetsu T, Kobashi K, Kakuta T. Ventricular Fibrillation During Optical Coherence Tomography/Optical Frequency Domain Imaging-A Large Single-Center Experience. Circ J 2020;84(2):178–185. [PubMed: 31941850]

9. Tearney GJ, Regar E, Akasaka T, Adriaenssens T, Barlis P, Bezerra HG, Bouma B, Bruining N, Cho JM, Chowdhary S, Costa MA, de Silva R, Dijkstra J, Di Mario C, Dudek D, Falk E, Feldman MD, Fitzgerald P, Garcia-Garcia HM, Gonzalo N, Granada JF, Guagliumi G, Holm NR, Honda Y, Ikeno F, Kawasaki M, Kochman J, Koltowski L, Kubo T, Kume T, Kyono H, Lam CC, Lamouche G, Lee DP, Leon MB, Maehara A, Manfrini O, Mintz GS, Mizuno K, Morel MA, Nadkarni S, Okura H, Otake H, Pietrasik A, Prati F, Raber L, Radu MD, Rieber J, Riga M, Rollins A, Rosenberg M, Sirbu V, Serruys PW, Shimada K, Shinke T, Shite J, Siegel E, Sonoda S, Suter M, Takarada S, Tanaka A, Terashima M, Thim T, Uemura S, Ughi GJ, van Beusekom HM, van der Steen AF, van Es GA, van Soest G, Virmani R, Waxman S, Weissman NJ, Weisz G, International Working Group for Intravascular Optical Coherence T. Consensus standards for acquisition, measurement, and reporting of intravascular optical coherence tomography studies: a report from the International Working Group for Intravascular Optical Coherence Tomography Standardization and Validation. J Am Coll Cardiol 2012;59(12):1058–72. [PubMed: 22421299]

10. Kubo T, Akasaka T, Shite J, Suzuki T, Uemura S, Yu B, Kozuma K, Kitabata H, Shinke T, Habara M, Saito Y, Hou J, Suzuki N, Zhang S. OCT compared with IVUS in a coronary lesion assessment: the OPUS-CLASS study. JACC Cardiovasc Imaging 2013;6(10):1095–1104. [PubMed: 24011777]

11. Gerbaud E, Weisz G, Tanaka A, Kashiwagi M, Shimizu T, Wang L, Souza C, Bouma BE, Suter MJ, Shishkov M, Ughi GJ, Halpern EF, Rosenberg M, Waxman S, Moses JW, Mintz GS, Maehara A, Tearney GJ. Multi-laboratory inter-institute reproducibility study of IVOCT and IVUS assessments using published consensus document definitions. Eur Heart J Cardiovasc Imaging 2016;17(7):756–64. [PubMed: 26377904]

12. Gonzalo N, Garcia-Garcia HM, Serruys PW, Commissaris KH, Bezerra H, Gobbens P, Costa M, Regar E. Reproducibility of quantitative optical coherence tomography for stent analysis. EuroIntervention 2009;5(2):224–32. [PubMed: 19527980]
13. Okamura T, Gonzalo N, Gutierrez-Chico JL, Serruys PW, Bruining N, de Winter S, Dijkstra J, Commossaris KH, van Geuns RJ, van Soest G, Ligthart J, Regar E. Reproducibility of coronary Fourier domain optical coherence tomography: quantitative analysis of in vivo stented coronary arteries using three different software packages. EuroIntervention 2010;6(3):371–9. [PubMed: 20884417]
14. Terashima M, Rathore S, Suzuki Y, Nakayama Y, Kaneda H, Nasu K, Habara M, Katoh O, Suzuki T. Accuracy and reproducibility of stent-strut thickness determined by optical coherence tomography. J Invasive Cardiol 2009;21(11):602–5. [PubMed: 19901417]
15. Kini AS, Vengrenyuk Y, Yoshimura T, Matsumura M, Pena J, Baber U, Moreno P, Mehran R, Maehara A, Sharma S, Narula J. Fibrous Cap Thickness by Optical Coherence Tomography In Vivo. J Am Coll Cardiol 2017;69(6):644–657. [PubMed: 27989887]
16. Tuzcu EM, Kapadia SR, Tutar E, Ziada KM, Hobbs RE, McCarthy PM, Young JB, Nissen SE. High prevalence of coronary atherosclerosis in asymptomatic teenagers and young adults: evidence from intravascular ultrasound. Circulation 2001;103(22):2705–10. [PubMed: 11390341]
17. Kume T, Okura H, Kawamoto T, Yamada R, Miyamoto Y, Hayashida A, Watanabe N, Neishi Y, Sadahira Y, Akasaka T, Yoshida K. Assessment of the coronary calcification by optical coherence tomography. EuroIntervention 2011;6(6):768–72. [PubMed: 21205603]
18. Saita T, Fujii K, Hao H, Imanaka T, Shibuya M, Fukunaga M, Miki K, Tamaru H, Horimatsu T, Nishimura M, Sumiyoshi A, Kawakami R, Naito Y, Kajimoto N, Hirota S, Masuyama T. Histopathological validation of optical frequency domain imaging to quantify various types of coronary calcifications. Eur Heart J Cardiovasc Imaging 2017;18(3):342–349. [PubMed: 27076364]
19. Kume T, Akasaka T, Kawamoto T, Watanabe N, Toyota E, Neishi Y, Sukmawan R, Sadahira Y, Yoshida K. Assessment of coronary arterial plaque by optical coherence tomography. Am J Cardiol 2006;97(8):1172–5. [PubMed: 16616021]
20. Kawasaki M, Bouma BE, Bressner J, Houser SL, Nadkarni SK, MacNeill BD, Jang IK, Fujiwara H, Tearney GJ. Diagnostic accuracy of optical coherence tomography and integrated backscatter intravascular ultrasound images for tissue characterization of human coronary plaques. J Am Coll Cardiol 2006;48(1):81–8. [PubMed: 16814652]
21. Kato K, Yonetsu T, Kim SJ, Xing L, Lee H, McNulty I, Yeh RW, Sakhuja R, Zhang S, Uemura S, Yu B, Mizuno K, Jang IK. Nonculprit plaques in patients with acute coronary syndromes have more vulnerable features compared with those with non-acute coronary syndromes: a 3-vessel optical coherence tomography study. Circ Cardiovasc Imaging 2012;5(4):433–40. [PubMed: 22679059]
22. Vergallo R, Uemura S, Soeda T, Minami Y, Cho JM, Ong DS, Aguirre AD, Gao L, Biasucci LM, Crea F, Yu B, Lee H, Kim CJ, Jang IK. Prevalence and Predictors of Multiple Coronary Plaque Ruptures: In Vivo 3-Vessel Optical Coherence Tomography Imaging Study. Arterioscler Thromb Vasc Biol 2016;36(11):2229–2238. [PubMed: 27634834]
23. Virmani R, Burke AP, Farb A, Kolodgie FD. Pathology of the vulnerable plaque. J Am Coll Cardiol 2006;47(8 Suppl):C13–8. [PubMed: 16631505]
24. Yonetsu T, Kakuta T, Lee T, Takahashi K, Kawaguchi N, Yamamoto G, Koura K, Hishikari K, Iesaka Y, Fujiwara H, Isobe M. In vivo critical fibrous cap thickness for rupture-prone coronary plaques assessed by optical coherence tomography. Eur Heart J 2011;32(10):1251–9. [PubMed: 21273202]
25. Radu MD, Yamaji K, Garcia-Garcia HM, Zaugg S, Taniwaki M, Koskinas KC, Serruys PW, Windecker S, Dijkstra J, Raber L. Variability in the measurement of minimum fibrous cap thickness and reproducibility of fibroatheroma classification by optical coherence tomography using manual versus semi-automatic assessment. EuroIntervention 2016;12(8):e987–e997. [PubMed: 27721214]
26. Galon MZ, Wang Z, Bezerra HG, Lemos PA, Schnell A, Wilson DL, Rollins AM, Costa MA, Attizzani GF. Differences determined by optical coherence tomography volumetric analysis in non-culprit lesion morphology and inflammation in ST-segment elevation myocardial infarction

and stable angina pectoris patients. Catheter Cardiovasc Interv 2015;85(4):E108–15. [PubMed: 25178981]

27. Tearney GJ, Yabushita H, Houser SL, Aretz HT, Jang IK, Schlendorf KH, Kauffman CR, Shishkov M, Halpern EF, Bouma BE. Quantification of macrophage content in atherosclerotic plaques by optical coherence tomography. Circulation 2003;107(1):113–9. [PubMed: 12515752]
28. Raber L, Koskinas KC, Yamaji K, Taniwaki M, Roffi M, Holmvang L, Garcia Garcia HM, Zanchin T, Maldonado R, Moschovitis A, Pedrazzini G, Zaugg S, Dijkstra J, Matter CM, Serruys PW, Luscher TF, Kelbaek H, Karagiannis A, Radu MD, Windecker S. Changes in Coronary Plaque Composition in Patients With Acute Myocardial Infarction Treated With High-Intensity Statin Therapy (IBIS-4): A Serial Optical Coherence Tomography Study. JACC Cardiovasc Imaging 2018;12(8 Pt 1):1518–1528. [PubMed: 30553686]
29. Di Vito L, Agozzino M, Marco V, Ricciardi A, Concardi M, Romagnoli E, Gatto L, Calogero G, Tavazzi L, Arbustini E, Prati F. Identification and quantification of macrophage presence in coronary atherosclerotic plaques by optical coherence tomography. Eur Heart J Cardiovasc Imaging 2015;16(7):807–13. [PubMed: 25588802]
30. Tahara S, Morooka T, Wang Z, Bezerra HG, Rollins AM, Simon DI, Costa MA. Intravascular optical coherence tomography detection of atherosclerosis and inflammation in murine aorta. Arterioscler Thromb Vasc Biol 2012;32(5):1150–7. [PubMed: 22308042]
31. Komukai K, Kubo T, Kitabata H, Matsuo Y, Ozaki Y, Takarada S, Okumoto Y, Shiono Y, Orii M, Shimamura K, Ueno S, Yamano T, Tanimoto T, Ino Y, Yamaguchi T, Kumiko H, Tanaka A, Imanishi T, Akagi H, Akasaka T. Effect of atorvastatin therapy on fibrous cap thickness in coronary atherosclerotic plaque as assessed by optical coherence tomography: the EASY-FIT study. J Am Coll Cardiol 2014;64(21):2207–17. [PubMed: 25456755]
32. Kolodgie FD, Gold HK, Burke AP, Fowler DR, Kruth HS, Weber DK, Farb A, Guerrero LJ, Hayase M, Kutys R, Narula J, Finn AV, Virmani R. Intraplaque hemorrhage and progression of coronary atheroma. N Engl J Med 2003;349(24):2316–25. [PubMed: 14668457]
33. Kume T, Okura H, Yamada R, Koyama T, Fukuhara K, Kawamura A, Imai K, Neishi Y, Uemura S. Detection of Plaque Neovascularization by Optical Coherence Tomography: Ex Vivo Feasibility Study and In Vivo Observation in Patients With Angina Pectoris. J Invasive Cardiol 2016;28(1):17–22. [PubMed: 26716590]
34. Nishimiya K, Matsumoto Y, Takahashi J, Uzuka H, Odaka Y, Nihei T, Hao K, Tsuburaya R, Ito K, Shimokawa H. In vivo visualization of adventitial vasa vasorum of the human coronary artery on optical frequency domain imaging. Validation study. Circ J 2014;78(10):2516–8. [PubMed: 24976390]
35. Aoki T, Rodriguez-Porcel M, Matsuo Y, Cassar A, Kwon TG, Franchi F, Gulati R, Kushwaha SS, Lennon RJ, Lerman LO, Ritman EL, Lerman A. Evaluation of coronary adventitial vasa vasorum using 3D optical coherence tomography--animal and human studies. Atherosclerosis 2015;239(1):203–8. [PubMed: 25618027]
36. Abela GS, Aziz K. Cholesterol crystals rupture biological membranes and human plaques during acute cardiovascular events--a novel insight into plaque rupture by scanning electron microscopy. Scanning 2006;28(1):1–10. [PubMed: 16502619]
37. Abela GS, Vedre A, Janoudi A, Huang R, Durga S, Tamhane U. Effect of statins on cholesterol crystallization and atherosclerotic plaque stabilization. Am J Cardiol 2011;107(12):1710–7. [PubMed: 21507364]
38. Crea F, Liuzzo G. Pathogenesis of acute coronary syndromes. J Am Coll Cardiol 2013;61(1):1–11. [PubMed: 23158526]
39. Katayama Y, Tanaka A, Taruya A, Kashiwagi M, Nishiguchi T, Ozaki Y, Matsuo Y, Kitabata H, Kubo T, Shimada E, Kondo T, Akasaka T. Feasibility and Clinical Significance of In Vivo Cholesterol Crystal Detection Using Optical Coherence Tomography. Arterioscler Thromb Vasc Biol 2020;40(1):220–229. [PubMed: 31619064]
40. Jinnouchi H, Sato Y, Torii S, Sakamoto A, Cornelissen A, Bhoite RR, Kuntz S, Guo L, Paek KH, Fernandez R, Kolodgie FD, Virmani R, Finn AV. Detection of cholesterol crystals by optical coherence tomography. EuroIntervention 2020;16(5):395–403. [PubMed: 32310132]

41. Kang SJ, Nakano M, Virmani R, Song HG, Ahn JM, Kim WJ, Lee JY, Park DW, Lee SW, Kim YH, Lee CW, Park SW, Park SJ. OCT findings in patients with recanalization of organized thrombi in coronary arteries. JACC Cardiovasc Imaging 2012;5(7):725–32. [PubMed: 22789941]

42. Souteyrand G, Valladier M, Amabile N, Derimay F, Harbaoui B, Leddet P, Barnay P, Malcles G, Mulliez A, Berry C, Eschalier R, Combaret N, Motreff P. Diagnosis and Management of Spontaneously Recanalized Coronary Thrombus Guided by Optical Coherence Tomography-Lessons From the French "Lotus Root" Registry. Circ J 2018;82(3):783–790. [PubMed: 29199266]

43. Prati F, Guagliumi G, Mintz GS, Costa M, Regar E, Akasaka T, Barlis P, Tearney GJ, Jang IK, Arbustini E, Bezerra HG, Ozaki Y, Bruining N, Dudek D, Radu M, Erglis A, Motreff P, Alfonso F, Toutouzas K, Gonzalo N, Tamburino C, Adriaenssens T, Pinto F, Serruys PW, Di Mario C, Expert's OCTRD. Expert review document part 2: methodology, terminology and clinical applications of optical coherence tomography for the assessment of interventional procedures. Eur Heart J 2012;33(20):2513–20. [PubMed: 22653335]

44. Amabile N, Hammas S, Fradi S, Souteyrand G, Veugeois A, Belle L, Motreff P, Caussin C. Intra-coronary thrombus evolution during acute coronary syndrome: regression assessment by serial optical coherence tomography analyses. Eur Heart J Cardiovasc Imaging 2015;16(4):433–40. [PubMed: 25428947]

45. Kajander OA, Koistinen LS, Eskola M, Huhtala H, Bhindi R, Niemela K, Jolly SS, Sheth T, Investigators T-OS. Feasibility and repeatability of optical coherence tomography measurements of pre-stent thrombus burden in patients with STEMI treated with primary PCI. Eur Heart J Cardiovasc Imaging 2015;16(1):96–107. [PubMed: 25240168]

46. Burke AP, Kolodgie FD, Farb A, Weber DK, Malcom GT, Smialek J, Virmani R. Healed plaque ruptures and sudden coronary death: evidence that subclinical rupture has a role in plaque progression. Circulation 2001;103(7):934–40. [PubMed: 11181466]

47. Mann J, Davies MJ. Mechanisms of progression in native coronary artery disease: role of healed plaque disruption. Heart 1999;82(3):265–8. [PubMed: 10455072]

48. Otsuka F, Joner M, Prati F, Virmani R, Narula J. Clinical classification of plaque morphology in coronary disease. Nat Rev Cardiol 2014;11(7):379–89. [PubMed: 24776706]

49. Vergallo R, Crea F. Atherosclerotic Plaque Healing. N Engl J Med 2020;383(9):846–857. [PubMed: 32846063]

50. Shimokado A, Matsuo Y, Kubo T, Nishiguchi T, Taruya A, Teraguchi I, Shiono Y, Orii M, Tanimoto T, Yamano T, Ino Y, Hozumi T, Tanaka A, Muragaki Y, Akasaka T. In vivo optical coherence tomography imaging and histopathology of healed coronary plaques. Atherosclerosis 2018;275:35–42. [PubMed: 29859471]

51. Hoshino M, Yonetsu T, Yuki Y, Inoue K, Kanaji Y, Usui E, Lee T, Kakuta T. Optical Coherence Tomographic Features of Unstable Coronary Lesions Corresponding to Histopathological Intraplaque Hemorrhage Evaluated by Directional Coronary Atherectomy Specimens. JACC Cardiovasc Interv 2018;11(14):1414–1415. [PubMed: 29960754]

52. Antuna P, Cuesta J, Bastante T, Montes A, Rivero F, Alfonso F. Diagnosis of Intraplaque Hemorrhage by High-Definition Intravascular Ultrasound and Optical Coherence Tomography. JACC Cardiovasc Interv 2020;13(16):1960–1962. [PubMed: 32739297]

53. Gerbaud E, Weisz G, Tanaka A, Luu R, Osman H, Baldwin G, Coste P, Cognet L, Waxman S, Zheng H, Moses JW, Mintz GS, Akasaka T, Maehara A, Tearney GJ. Plaque burden can be assessed using intravascular optical coherence tomography and a dedicated automated processing algorithm: a comparison study with intravascular ultrasound. Eur Heart J Cardiovasc Imaging 2019;21(6):640–652.

54. Ramasamy A, Ng J, White S, Johnson TW, Foin N, Girard MJA, Dijkstra J, Amersey R, Scoltock S, Koganti S, Jones D, Jin C, Raber L, Serruys PW, Torii R, Crake T, Rakhit R, Baumbach A, Mathur A, Bourantas CV. Efficacy and Reproducibility of Attenuation-Compensated Optical Coherence Tomography for Assessing External Elastic Membrane Border and Plaque Composition in Native and Stented Segments-An In Vivo and Histology-Based Study. Circ J 2019;84(1):91–100. [PubMed: 31735729]

55. Kubo T, Imanishi T, Takarada S, Kuroi A, Ueno S, Yamano T, Tanimoto T, Matsuo Y, Masho T, Kitabata H, Tsuda K, Tomobuchi Y, Akasaka T. Assessment of culprit lesion morphology in

acute myocardial infarction: ability of optical coherence tomography compared with intravascular ultrasound and coronary angioscopy. J Am Coll Cardiol 2007;50(10):933–9. [PubMed: 17765119]

56. Virmani R, Kolodgie FD, Burke AP, Farb A, Schwartz SM. Lessons from sudden coronary death: a comprehensive morphological classification scheme for atherosclerotic lesions. Arterioscler Thromb Vasc Biol 2000;20(5):1262–75. [PubMed: 10807742]
57. Jia H, Abtahian F, Aguirre AD, Lee S, Chia S, Lowe H, Kato K, Yonetsu T, Vergallo R, Hu S, Tian J, Lee H, Park SJ, Jang YS, Raffel OC, Mizuno K, Uemura S, Itoh T, Kakuta T, Choi SY, Dauerman HL, Prasad A, Toma C, McNulty I, Zhang S, Yu B, Fuster V, Narula J, Virmani R, Jang IK. In vivo diagnosis of plaque erosion and calcified nodule in patients with acute coronary syndrome by intravascular optical coherence tomography. J Am Coll Cardiol 2013;62(19):1748–58. [PubMed: 23810884]
58. Prati F, Uemura S, Souteyrand G, Virmani R, Motreff P, Di Vito L, Biondi-Zoccai G, Halperin J, Fuster V, Ozaki Y, Narula J. OCT-based diagnosis and management of STEMI associated with intact fibrous cap. JACC Cardiovasc Imaging 2013;6(3):283–7. [PubMed: 23473109]
59. Jia H, Dai J, Hou J, Xing L, Ma L, Liu H, Xu M, Yao Y, Hu S, Yamamoto E, Lee H, Zhang S, Yu B, Jang IK. Effective anti-thrombotic therapy without stenting: intravascular optical coherence tomography-based management in plaque erosion (the EROSION study). Eur Heart J 2017;38(11):792–800. [PubMed: 27578806]
60. Xing L, Yamamoto E, Sugiyama T, Jia H, Ma L, Hu S, Wang C, Zhu Y, Li L, Xu M, Liu H, Bryniarski K, Hou J, Zhang S, Lee H, Yu B, Jang IK. EROSION Study (Effective Anti-Thrombotic Therapy Without Stenting: Intravascular Optical Coherence Tomography-Based Management in Plaque Erosion): A 1-Year Follow-Up Report. Circ Cardiovasc Interv 2017;10(12).
61. Luping H, Yuhan Q, Yishuo X, Sining H, Yini W, Ming Z, Xue F, Qi L, Ikramullah S, Abigail D, Chen Z, Xi C, Zhaoyue L, Wei M, Maoen X, Huimin L, Lijia M, Jiannan D, Lei X, Huai Y, Jingbo H, Haibo J, Gary SM, Bo Y. Predictors of Non-Stenting Strategy for Acute Coronary Syndrome Caused by Plaque Erosion: 4-Year Outcomes of the EROSION Study. EuroIntervention 2020.
62. Combaret N, Souteyrand G, Barber-Chamoux N, Malcles G, Amonchot A, Pereira B, Le Bivic L, Eschalier R, Trésorier R, Motreff P. Management of ST-elevation myocardial infarction in young patients by limiting implantation of durable intracoronary devices and guided by optical frequency domain imaging: “proof of concept” study. EuroIntervention 2017;13(4):397–406. [PubMed: 28067196]
63. Torii S, Sato Y, Otsuka F, Kolodgie FD, Jinnouchi H, Sakamoto A, Park J, Yahagi K, Sakakura K, Cornelissen A, Kawakami R, Mori M, Kawai K, Amoa F, Guo L, Kutyna M, Fernandez R, Romero ME, Fowler D, Finn AV, Virmani R. Eruptive Calcified Nodules as a Potential Mechanism of Acute Coronary Thrombosis and Sudden Death. Journal of the American College of Cardiology 2021;77(13):1599–1611. [PubMed: 33795033]
64. Kobayashi N, Takano M, Tsurumi M, Shibata Y, Nishigoori S, Uchiyama S, Okazaki H, Shirakabe A, Seino Y, Hata N, Shimizu W. Features and Outcomes of Patients with Calcified Nodules at Culprit Lesions of Acute Coronary Syndrome: An Optical Coherence Tomography Study. Cardiology 2018;139(2):90–100. [PubMed: 29301128]
65. Prati F, Gatto L, Fabbiocchi F, Vergallo R, Paoletti G, Ruscica G, Marco V, Romagnoli E, Boi A, Fineschi M, Calligaris G, Tamburino C, Crea F, Ozaki Y, Alfonso F, Arbustini E. Clinical outcomes of calcified nodules detected by optical coherence tomography: a sub-analysis of the CLIMA study. EuroIntervention 2020;16(5):380–386. [PubMed: 32310133]
66. Sugiyama T, Yamamoto E, Fracassi F, Lee H, Yonetsu T, Kakuta T, Soeda T, Saito Y, Yan BP, Kurihara O, Takano M, Niccoli G, Crea F, Higuma T, Kimura S, Minami Y, Ako J, Adriaenssens T, Boeder NF, Nef HM, Fujimoto JG, Fuster V, Finn AV, Falk E, Jang IK. Calcified Plaques in Patients With Acute Coronary Syndromes. JACC Cardiovasc Interv 2019;12(6):531–540. [PubMed: 30898249]
67. Mortensen KH, Thuesen L, Kristensen IB, Christiansen EH. Spontaneous coronary artery dissection: a Western Denmark Heart Registry study. Catheter Cardiovasc Interv 2009;74(5):710–7. [PubMed: 19496145]

68. Nishiguchi T, Tanaka A, Ozaki Y, Taruya A, Fukuda S, Taguchi H, Iwaguro T, Ueno S, Okumoto Y, Akasaka T. Prevalence of spontaneous coronary artery dissection in patients with acute coronary syndrome. Eur Heart J Acute Cardiovasc Care 2016;5(3):263–70. [PubMed: 24585938]

69. Saw J, Starovoytov A, Humphries K, Sheth T, So D, Minhas K, Brass N, Lavoie A, Bishop H, Lavi S, Pearce C, Renner S, Madan M, Welsh RC, Lutchmedial S, Vijayaraghavan R, Aymong E, Har B, Ibrahim R, Gornik HL, Ganesh S, Buller C, Matteau A, Martucci G, Ko D, Mancini GBJ. Canadian spontaneous coronary artery dissection cohort study: in-hospital and 30-day outcomes. Eur Heart J 2019;40(15):1188–1197. [PubMed: 30698711]

70. Saw J Coronary angiogram classification of spontaneous coronary artery dissection. Catheter Cardiovasc Interv 2014;84(7):1115–22. [PubMed: 24227590]

71. Tamis-Holland JE, Jneid H, Reynolds HR, Agewall S, Brilakis ES, Brown TM, Lerman A, Cushman M, Kumbhani DJ, Arslanian-Engoren C, Bolger AF, Beltrame JF, American Heart Association Interventional Cardiovascular Care Committee of the Council on Clinical C, Council on C, Stroke N, Council on E, Prevention, Council on Quality of C, Outcomes R. Contemporary Diagnosis and Management of Patients With Myocardial Infarction in the Absence of Obstructive Coronary Artery Disease: A Scientific Statement From the American Heart Association. Circulation 2019;139(18):e891–e908. [PubMed: 30913893]

72. Opolski MP, Spiewak M, Marczak M, Debski A, Knaapen P, Schumacher SP, Staruch AD, Grodecki K, Chmielak Z, Lazarczyk H, Kukula K, Tyczynski P, Pregowski J, Dabrowski M, Kadziela J, Florczak E, Skrobisz A, Witkowski A. Mechanisms of Myocardial Infarction in Patients With Nonobstructive Coronary Artery Disease: Results From the Optical Coherence Tomography Study. JACC Cardiovasc Imaging 2019;12(11 Pt 1):2210–2221. [PubMed: 30343070]

73. Gerbaud E, Arabucki F, Nivet H, Barbey C, Cetran L, Chassaing S, Seguy B, Lesimple A, Cochet H, Montaudon M, Laurent F, Bar O, Tearney GJ, Coste P. OCT and CMR for the Diagnosis of Patients Presenting With MINOCA and Suspected Epicardial Causes. JACC Cardiovasc Imaging 2020;13(12):2619–2631. [PubMed: 32828786]

74. Reynolds HR, Maehara A, Kwong RY, Sedlak T, Saw J, Smilowitz NR, Mahmud E, Wei J, Marzo K, Matsumura M, Seno A, Hausvater A, Giesler C, Jhalani N, Toma C, Har B, Thomas D, Mehta LS, Trost J, Mehta PK, Ahmed B, Bainey KR, Xia Y, Shah B, Attubato M, Bangalore S, Razzouk L, Ali ZA, Merz NB, Park K, Hada E, Zhong H, Hochman JS. Coronary Optical Coherence Tomography and Cardiac Magnetic Resonance Imaging to Determine Underlying Causes of Myocardial Infarction With Nonobstructive Coronary Arteries in Women. Circulation 2021;143(7):624–640. [PubMed: 33191769]

75. Jang IK. Pursuit for the detection of vulnerable plaque. Eur Heart J 2020;41(3):392–393. [PubMed: 31549717]

76. Belguidoum S, Meneveau N, Motreff P, Ohlman P, Boussaada MM, Silvain J, Guillon B, Descotes-Genon V, Lefrançois Y, Morel O, Amabile N. Relationship between stent expansion and fractional flow reserve after percutaneous coronary intervention: a post hoc analysis of the DOCTORS trial. EuroIntervention 2021;17(2):e132–e139. [PubMed: 32392171]

77. Prati F, Romagnoli E, Burzotta F, Limbruno U, Gatto L, La Manna A, Versaci F, Marco V, Di Vito L, Imola F, Paoletti G, Trani C, Tamburino C, Tavazzi L, Mintz GS. Clinical Impact of OCT Findings During PCI: The CLI-OPCI II Study. JACC Cardiovasc Imaging 2015;8(11):1297–305. [PubMed: 26563859]

78. Soeda T, Uemura S, Park SJ, Jang Y, Lee S, Cho JM, Kim SJ, Vergallo R, Minami Y, Ong DS, Gao L, Lee H, Zhang S, Yu B, Saito Y, Jang IK. Incidence and Clinical Significance of Poststent Optical Coherence Tomography Findings: One-Year Follow-Up Study From a Multicenter Registry. Circulation 2015;132(11):1020–9. [PubMed: 26162917]

79. Meneveau N, Souteyrand G, Motreff P, Caussin C, Amabile N, Ohlmann P, Morel O, Lefrancois Y, Descotes-Genon V, Silvain J, Braik N, Chopard R, Chatot M, Ecarnot F, Tauzin H, Van Belle E, Belle L, Schiele F. Optical Coherence Tomography to Optimize Results of Percutaneous Coronary Intervention in Patients with Non-ST-Elevation Acute Coronary Syndrome: Results of the Multicenter, Randomized DOCTORS Study (Does Optical Coherence Tomography Optimize Results of Stenting). Circulation 2016;134(13):906–17. [PubMed: 27573032]

80. Antonsen L, Thayssen P, Maehara A, Hansen HS, Junker A, Veien KT, Hansen KN, Hougaard M, Mintz GS, Jensen LO. Optical Coherence Tomography Guided Percutaneous Coronary

Intervention With Nobori Stent Implantation in Patients With Non-ST-Segment-Elevation Myocardial Infarction (OCTACS) Trial: Difference in Strut Coverage and Dynamic Malapposition Patterns at 6 Months. Circ Cardiovasc Interv 2015;8(8):e002446. [PubMed: 26253735]

81. Ali ZA, Maehara A, Genereux P, Shlofmitz RA, Fabbiocchi F, Nazif TM, Guagliumi G, Meraj PM, Alfonso F, Samady H, Akasaka T, Carlson EB, Leesar MA, Matsumura M, Ozan MO, Mintz GS, Ben-Yehuda O, Stone GW, Investigators IIOP. Optical coherence tomography compared with intravascular ultrasound and with angiography to guide coronary stent implantation (ILUMIEN III: OPTIMIZE PCI): a randomised controlled trial. Lancet 2016;388(10060):2618–2628. [PubMed: 27806900]
82. Kubo T, Shinke T, Okamura T, Hibi K, Nakazawa G, Morino Y, Shite J, Fusazaki T, Otake H, Kozuma K, Ioji T, Kaneda H, Serikawa T, Kataoka T, Okada H, Akasaka T, Investigators O. Optical frequency domain imaging vs. intravascular ultrasound in percutaneous coronary intervention (OPINION trial): one-year angiographic and clinical results. Eur Heart J 2017;38(42):3139–3147. [PubMed: 29121226]
83. Adriaenssens T, Joner M, Godschalk TC, Malik N, Alfonso F, Xhepa E, De Cock D, Komukai K, Tada T, Cuesta J, Sirbu V, Feldman LJ, Neumann FJ, Goodall AH, Heestermans T, Buysschaert I, Hlinomaz O, Belmans A, Desmet W, Ten Berg JM, Gershlick AH, Massberg S, Kastrati A, Guagliumi G, Byrne RA, Prevention of Late Stent Thrombosis by an Interdisciplinary Global European Effort I. Optical Coherence Tomography Findings in Patients With Coronary Stent Thrombosis: A Report of the PRESTIGE Consortium (Prevention of Late Stent Thrombosis by an Interdisciplinary Global European Effort). Circulation 2017;136(11):1007–1021. [PubMed: 28720725]
84. Souteyrand G, Amabile N, Mangin L, Chabin X, Meneveau N, Cayla G, Vanzetto G, Barnay P, Trouillet C, Rioufol G, Range G, Teiger E, Delaunay R, Dubreuil O, Lhermusier T, Mulliez A, Levesque S, Belle L, Caussin C, Motreff P, Investigators P. Mechanisms of stent thrombosis analysed by optical coherence tomography: insights from the national PESTO French registry. Eur Heart J 2016;37(15):1208–16. [PubMed: 26757787]
85. Prati F, Romagnoli E, Gatto L, La Manna A, Burzotta F, Limbruno U, Versaci F, Fabbiocchi F, Di Giorgio A, Marco V, Ramazzotti V, Di Vito L, Trani C, Porto I, Boi A, Tavazzi L, Mintz GS. Clinical Impact of Suboptimal Stenting and Residual Intrastent Plaque/Thrombus Protrusion in Patients With Acute Coronary Syndrome: The CLI-OPCI ACS Substudy (Centro per la Lotta Contro L'Infarto-Optimization of Percutaneous Coronary Intervention in Acute Coronary Syndrome). Circ Cardiovasc Interv 2016;9(12).
86. Kawamori H, Shite J, Shinke T, Otake H, Matsumoto D, Nakagawa M, Nagoshi R, Kozuki A, Hariki H, Inoue T, Osue T, Taniguchi Y, Nishio R, Hiranuma N, Hirata K. Natural consequence of post-intervention stent malapposition, thrombus, tissue prolapse, and dissection assessed by optical coherence tomography at mid-term follow-up. Eur Heart J Cardiovasc Imaging 2013;14(9):865–75. [PubMed: 23291393]
87. Radu MD, Raber L, Heo J, Gogas BD, Jorgensen E, Kelbaek H, Muramatsu T, Farooq V, Helqvist S, Garcia-Garcia HM, Windecker S, Saunamaki K, Serruys PW. Natural history of optical coherence tomography-detected non-flow-limiting edge dissections following drug-eluting stent implantation. EuroIntervention 2014;9(9):1085–94. [PubMed: 24064426]
88. Kubo T, Shimamura K, Ino Y, Yamaguchi T, Matsuo Y, Shiono Y, Taruya A, Nishiguchi T, Shimokado A, Teraguchi I, Orii M, Yamano T, Tanimoto T, Kitabata H, Hirata K, Tanaka A, Akasaka T. Superficial Calcium Fracture After PCI as Assessed by OCT. JACC Cardiovasc Imaging 2015;8(10):1228–1229. [PubMed: 25797130]
89. Imola F, Occhipinti M, Biondi-Zoccai G, Di Vito L, Ramazzotti V, Manzoli A, Pappalardo A, Cremonesi A, Albertucci M, Prati F. Association between proximal stent edge positioning on atherosclerotic plaques containing lipid pools and postprocedural myocardial infarction (from the CLI-POOL Study). Am J Cardiol 2013;111(4):526–31. [PubMed: 23206925]
90. Ino Y, Kubo T, Matsuo Y, Yamaguchi T, Shiono Y, Shimamura K, Katayama Y, Nakamura T, Aoki H, Taruya A, Nishiguchi T, Satogami K, Yamano T, Kameyama T, Orii M, Ota S, Kuroi A, Kitabata H, Tanaka A, Hozumi T, Akasaka T. Optical Coherence Tomography Predictors for Edge Restenosis After Everolimus-Eluting Stent Implantation. Circ Cardiovasc Interv 2016;9(10).

91. Neumann FJ, Sousa-Uva M, Ahlsson A, Alfonso F, Banning AP, Benedetto U, Byrne RA, Collet JP, Falk V, Head SJ, Juni P, Kastrati A, Koller A, Kristensen SD, Niebauer J, Richter DJ, Seferovic PM, Sibbing D, Stefanini GG, Windecker S, Yadav R, Zembala MO, Group ESCSD. 2018 ESC/EACTS Guidelines on myocardial revascularization. Eur Heart J 2019;40(2):87–165. [PubMed: 30165437]

92. Fihn SD, Gardin JM, Abrams J, Berra K, Blankenship JC, Dallas AP, Douglas PS, Foody JM, Gerber TC, Hinderliter AL, King SB 3rd, Kligfield PD, Krumholz HM, Kwong RY, Lim MJ, Linderbaum JA, Mack MJ, Munger MA, Prager RL, Sabik JF, Shaw LJ, Sikkema JD, Smith CR Jr., Smith SC Jr., Spertus JA, Williams SV, American College of Cardiology F, American Heart Association Task Force on Practice G, American College of P, American Association for Thoracic S, Preventive Cardiovascular Nurses A, Society for Cardiovascular A, Interventions, Society of Thoracic S. 2012 ACCF/AHA/ACP/AATS/PCNA/SCAI/STS Guideline for the diagnosis and management of patients with stable ischemic heart disease: a report of the American College of Cardiology Foundation/American Heart Association Task Force on Practice Guidelines, and the American College of Physicians, American Association for Thoracic Surgery, Preventive Cardiovascular Nurses Association, Society for Cardiovascular Angiography and Interventions, and Society of Thoracic Surgeons. J Am Coll Cardiol 2012;60(24):e44–e164. [PubMed: 23182125]

93. Patel MR, Calhoon JH, Dehmer GJ, Grantham JA, Maddox TM, Maron DJ, Smith PK. ACC/AATS/AHA/ASE/ASNC/SCAI/SCCT/STS 2017 Appropriate Use Criteria for Coronary Revascularization in Patients With Stable Ischemic Heart Disease: A Report of the American College of Cardiology Appropriate Use Criteria Task Force, American Association for Thoracic Surgery, American Heart Association, American Society of Echocardiography, American Society of Nuclear Cardiology, Society for Cardiovascular Angiography and Interventions, Society of Cardiovascular Computed Tomography, and Society of Thoracic Surgeons. J Am Coll Cardiol 2017;69(17):2212–2241. [PubMed: 28291663]

94. Burzotta F, Leone AM, Aurigemma C, Zambrano A, Zimbardo G, Arioti M, Vergallo R, De Maria GL, Cerracchio E, Romagnoli E, Trani C, Crea F. Fractional Flow Reserve or Optical Coherence Tomography to Guide Management of Angiographically Intermediate Coronary Stenosis: A Single-Center Trial. JACC Cardiovasc Interv 2020;13(1):49–58. [PubMed: 31918942]

95. Kennedy MW, Fabris E, Ijsselmuiden AJ, Nef H, Reith S, Escaned J, Alfonso F, van Royen N, Wojakowski W, Witkowski A, Indolfi C, Ottervanger JP, Suryapranata H, Kedhi E. Combined optical coherence tomography morphologic and fractional flow reserve hemodynamic assessment of non-culprit lesions to better predict adverse event outcomes in diabetes mellitus patients: COMBINE (OCT-FFR) prospective study. Rationale and design. Cardiovasc Diabetol 2016;15(1):144. [PubMed: 27724869]

96. Burzotta F, Nerla R, Hill J, Paraggio L, Leone AM, Byrne J, Porto I, Niccoli G, Aurigemma C, Trani C, MacCarthy P, Crea F. Correlation between frequency-domain optical coherence tomography and fractional flow reserve in angiographically-intermediate coronary lesions. Int J Cardiol 2018;253:55–60. [PubMed: 29306471]

97. Lee JM, Choi KH, Koo BK, Zhang J, Han JK, Yang HM, Park KW, Song YB, Hahn JY, Choi SH, Gwon HC, Kim HS. Intravascular ultrasound or optical coherence tomography-defined anatomic severity and hemodynamic severity assessed by coronary physiologic indices. Rev Esp Cardiol (Engl Ed) 2020;73(10):812–821. [PubMed: 31812517]

98. Rivero F, Antuña P, García-Guimaraes M, Jiménez C, Cuesta J, Bastante T, Alfonso F. Correlation between fractional flow reserve and instantaneous wave-free ratio with morphometric assessment by optical coherence tomography in diabetic patients. Int J Cardiovasc Imaging 2020;36(7):1193–1201. [PubMed: 32221772]

99. Usui E, Yonetsu T, Kanaji Y, Hoshino M, Yamaguchi M, Hada M, Hamaya R, Kanno Y, Murai T, Lee T, Kakuta T. Efficacy of Optical Coherence Tomography-derived Morphometric Assessment in Predicting the Physiological Significance of Coronary Stenosis: Head-to-Head Comparison with Intravascular Ultrasound. EuroIntervention 2018;13(18):e2210–e2218. [PubMed: 29155383]

100. Ramasamy A, Chen Y, Zanchin T, Jones DA, Rathod K, Jin C, Onuma Y, Zhang YJ, Amersey R, Westwood M, Ozkor M, O'Mahony C, Lansky A, Crake T, Serruys PW, Mathur A, Baumbach A, Bourantas CV. Optical coherence tomography enables more accurate detection of functionally significant intermediate non-left main coronary artery stenoses than intravascular ultrasound: A

meta-analysis of 6919 patients and 7537 lesions. Int J Cardiol 2020;301:226–234. [PubMed: 31677827]

101. Huang J, Emori H, Ding D, Kubo T, Yu W, Huang P, Zhang S, Gutiérrez-Chico JL, Akasaka T, Wijns W, Tu S. Diagnostic performance of intracoronary optical coherence tomography-based versus angiography-based fractional flow reserve for the evaluation of coronary lesions. EuroIntervention 2020;16(7):568–576. [PubMed: 31951207]
102. Yu W, Huang J, Jia D, Chen S, Raffel OC, Ding D, Tian F, Kan J, Zhang S, Yan F, Chen Y, Bezerra HG, Wijns W, Tu S. Diagnostic accuracy of intracoronary optical coherence tomography-derived fractional flow reserve for assessment of coronary stenosis severity. EuroIntervention 2019;15(2):189–197. [PubMed: 31147309]
103. Ding D, Yu W, Tauzin H, De Maria GL, Wu P, Yang F, Kotronias RA, Terentes-Printzios D, Wolfrum M, Banning AP, Meneveau N, Wijns W, Tu S. Optical Flow Ratio for Assessing Stenting Result and Physiological Significance of Residual Disease. EuroIntervention 2021.
104. Burzotta F, Lassen JF, Lefevre T, Banning AP, Chatzizisis YS, Johnson TW, Ferenc M, Rathore S, Albiero R, Pan M, Darremont O, Hildick-Smith D, Chieffo A, Zimarino M, Louvard Y, Stankovic G. Percutaneous coronary intervention for bifurcation coronary lesions: the 15(th) consensus document from the European Bifurcation Club. EuroIntervention 2021;16(16):1307–1317. [PubMed: 33074152]
105. Holm NR, Andreasen LN, Walsh S, Kajander OA, Witt N, Eek C, Knaapen P, Koltowski L, Gutiérrez-Chico JL, Burzotta F, Kockman J, Ormiston J, Santos-Pardo I, Laanmets P, Mylotte D, Madsen M, Hjort J, Kumsars I, Råmunddal T, Christiansen EH. Rational and design of the European randomized Optical Coherence Tomography Optimized Bifurcation Event Reduction Trial (OCTOBER). Am Heart J 2018;205:97–109. [PubMed: 30205242]
106. Onuma Y, Kogame N, Sotomi Y, Miyazaki Y, Asano T, Takahashi K, Kawashima H, Ono M, Katagiri Y, Kyono H, Nakatani S, Muramatsu T, Sharif F, Ozaki Y, Serruys PW, Okamura T, Investigators O. A Randomized Trial Evaluating Online 3-Dimensional Optical Frequency Domain Imaging-Guided Percutaneous Coronary Intervention in Bifurcation Lesions. Circ Cardiovasc Interv 2020;13(12):e009183. [PubMed: 33272034]
107. Amabile N, Rangé G, Souteyrand G, Godin M, Boussaada MM, Meneveau N, Cayla G, Casassus F, Lefèvre T, Hakim R, Bagdadi I, Motreff P, Caussin C. Optical coherence tomography to guide percutaneous coronary intervention of the left main coronary artery: the LEMON study. EuroIntervention 2021;17(2):e124–e131. [PubMed: 33226003]
108. Onuma Y, Katagiri Y, Burzotta F, Holm NR, Amabile N, Okamura T, Mintz GS, Darremont O, Lassen JF, Lefevre T, Louvard Y, Stankovic G, Serruys PW. Joint consensus on the use of OCT in coronary bifurcation lesions by the European and Japanese bifurcation clubs. EuroIntervention 2019;14(15):e1568–e1577. [PubMed: 30479307]
109. Templin C, Meyer M, Muller MF, Djonov V, Hlushchuk R, Dimova I, Flueckiger S, Kronen P, Sidler M, Klein K, Nicholls F, Ghadri JR, Weber K, Paunovic D, Corti R, Hoerstrup SP, Luscher TF, Landmesser U. Coronary optical frequency domain imaging (OFDI) for in vivo evaluation of stent healing: comparison with light and electron microscopy. Eur Heart J 2010;31(14):1792–801. [PubMed: 20525979]
110. Jinnouchi H, Otsuka F, Sato Y, Bhoite RR, Sakamoto A, Torii S, Yahagi K, Cornelissen A, Mori M, Kawakami R, Kolodgie FD, Virmani R, Finn AV. Healthy Strut Coverage After Coronary Stent Implantation: An Ex Vivo Human Autopsy Study. Circ Cardiovasc Interv 2020;13(5):e008869. [PubMed: 32338525]
111. Radu MD, Raber L, Kalesan B, Muramatsu T, Kelbaek H, Heo J, Jorgensen E, Helqvist S, Farooq V, Brugaletta S, Garcia-Garcia HM, Juni P, Saunamaki K, Windecker S, Serruys PW. Coronary evaginations are associated with positive vessel remodelling and are nearly absent following implantation of newer-generation drug-eluting stents: an optical coherence tomography and intravascular ultrasound study. Eur Heart J 2014;35(12):795–807. [PubMed: 24132187]
112. Xhepa E, Bresha J, Joner M, Hapfelmeier A, Rivero F, Ndrepepa G, Nano N, Cuesta J, Kufner S, Cassese S, Bastante T, Aytekin A, Rroku A, Garcia-Guimaraes M, Lahmann AL, Pinieck S, Rai H, Fusaro M, Schunkert H, Perez-Vizcayno MJ, Gonzalo N, Alfonso F, Kastrati A. Clinical outcomes by optical characteristics of neointima and treatment modality in patients with coronary in-stent restenosis. EuroIntervention 2020.

113. Madhavan MV, Kirtane AJ, Redfors B, Genereux P, Ben-Yehuda O, Palmerini T, Benedetto U, Biondi-Zoccai G, Smits PC, von Birgelen C, Mehran R, McAndrew T, Serruys PW, Leon MB, Pocock SJ, Stone GW. Stent-Related Adverse Events >1 Year After Percutaneous Coronary Intervention. J Am Coll Cardiol 2020;75(6):590–604. [PubMed: 32057373]

114. Takano M, Yamamoto M, Inami S, Murakami D, Ohba T, Seino Y, Mizuno K. Appearance of lipid-laden intima and neovascularization after implantation of bare-metal stents extended late-phase observation by intracoronary optical coherence tomography. J Am Coll Cardiol 2009;55(1):26–32. [PubMed: 20117359]

115. Nakazawa G, Otsuka F, Nakano M, Vorpahl M, Yazdani SK, Ladich E, Kolodgie FD, Finn AV, Virmani R. The pathology of neoatherosclerosis in human coronary implants bare-metal and drug-eluting stents. J Am Coll Cardiol 2011;57(11):1314–22. [PubMed: 21376502]

116. Yonetsu T, Kim JS, Kato K, Kim SJ, Xing L, Yeh RW, Sakhuja R, McNulty I, Lee H, Zhang S, Uemura S, Yu B, Kakuta T, Jang IK. Comparison of incidence and time course of neoatherosclerosis between bare metal stents and drug-eluting stents using optical coherence tomography. Am J Cardiol 2012;110(7):933–9. [PubMed: 22727183]

117. Amabile N, Souteyrand G, Ghostine S, Combaret N, Slama MS, Barber-Chamoux N, Motreff P, Caussin C. Very late stent thrombosis related to incomplete neointimal coverage or neoatherosclerotic plaque rupture identified by optical coherence tomography imaging. Eur Heart J Cardiovasc Imaging 2014;15(1):24–31. [PubMed: 23720378]

118. Taniwaki M, Radu MD, Zaugg S, Amabile N, Garcia-Garcia HM, Yamaji K, Jorgensen E, Kelbaek H, Pilgrim T, Caussin C, Zanchin T, Veugeois A, Abildgaard U, Juni P, Cook S, Koskinas KC, Windecker S, Raber L. Mechanisms of Very Late Drug-Eluting Stent Thrombosis Assessed by Optical Coherence Tomography. Circulation 2016;133(7):650–60. [PubMed: 26762519]

119. Souteyrand G, Amabile N, Mangin L, Chabin X, Meneveau N, Cayla G, Vanzetto G, Barnay P, Trouillet C, Rioufol G, Rangé G, Teiger E, Delaunay R, Dubreuil O, Lhermusier T, Mulliez A, Levesque S, Belle L, Caussin C, Motreff P. Mechanisms of stent thrombosis analysed by optical coherence tomography: insights from the national PESTO French registry. Eur Heart J 2016;37(15):1208–16. [PubMed: 26757787]

120. Hill JM, Kereiakes DJ, Shlofmitz RA, Klein AJ, Riley RF, Price MJ, Herrmann HC, Bachinsky W, Waksman R, Stone GW. Intravascular Lithotripsy for Treatment of Severely Calcified Coronary Artery Disease: The Disrupt CAD III Study. J Am Coll Cardiol 2020;76(22):2635–2646. [PubMed: 33069849]

121. Min HS, Yoo JH, Kang SJ, Lee JG, Cho H, Lee PH, Ahn JM, Park DW, Lee SW, Kim YH, Lee CW, Park SW, Park SJ. Detection of Optical Coherence Tomography-Defined Thin-Cap Fibroatheroma in the Coronary Artery Using Deep Learning. EuroIntervention 2019;16(5):404–412.

122. Chu M, Jia H, Gutiérrez-Chico JL, Maehara A, Ali ZA, Zeng X, He L, Zhao C, Matsumura M, Wu P, Zeng M, Kubo T, Xu B, Chen L, Yu B, Mintz GS, Wijns W, Holm NR, Tu S. Artificial intelligence and optical coherence tomography for the automatic characterisation of human atherosclerotic plaques. EuroIntervention 2021;17(1):41–50. [PubMed: 33528359]

123. Yin J, Yang HC, Li X, Zhang J, Zhou Q, Hu C, Shung KK, Chen Z. Integrated intravascular optical coherence tomography ultrasound imaging system. J Biomed Opt 2010;15(1):010512. [PubMed: 20210424]

124. Fard AM, Vacas-Jacques P, Hamidi E, Wang H, Carruth RW, Gardecki JA, Tearney GJ. Optical coherence tomography--near infrared spectroscopy system and catheter for intravascular imaging. Opt Express 2013;21(25):30849–58. [PubMed: 24514658]

125. Yoo H, Kim JW, Shishkov M, Namati E, Morse T, Shubochkin R, McCarthy JR, Ntziachristos V, Bouma BE, Jaffer FA, Tearney GJ. Intra-arterial catheter for simultaneous microstructural and molecular imaging in vivo. Nat Med 2011;17(12):1680–4. [PubMed: 22057345]

126. Park J, Jo JA, Shrestha S, Pande P, Wan Q, Applegate BE. A dual-modality optical coherence tomography and fluorescence lifetime imaging microscopy system for simultaneous morphological and biochemical tissue characterization. Biomed Opt Express 2010;1(1):186–200. [PubMed: 21258457]

127. Liu L, Gardecki JA, Nadkarni SK, Toussaint JD, Yagi Y, Bouma BE, Tearney GJ. Imaging the subcellular structure of human coronary atherosclerosis using micro-optical coherence tomography. Nat Med 2011;17(8):1010–4. [PubMed: 21743452]

128. de Boer JF, Hitzenberger CK, Yasuno Y. Polarization sensitive optical coherence tomography - a review [Invited]. Biomed Opt Express 2017;8(3):1838–1873. [PubMed: 28663869]

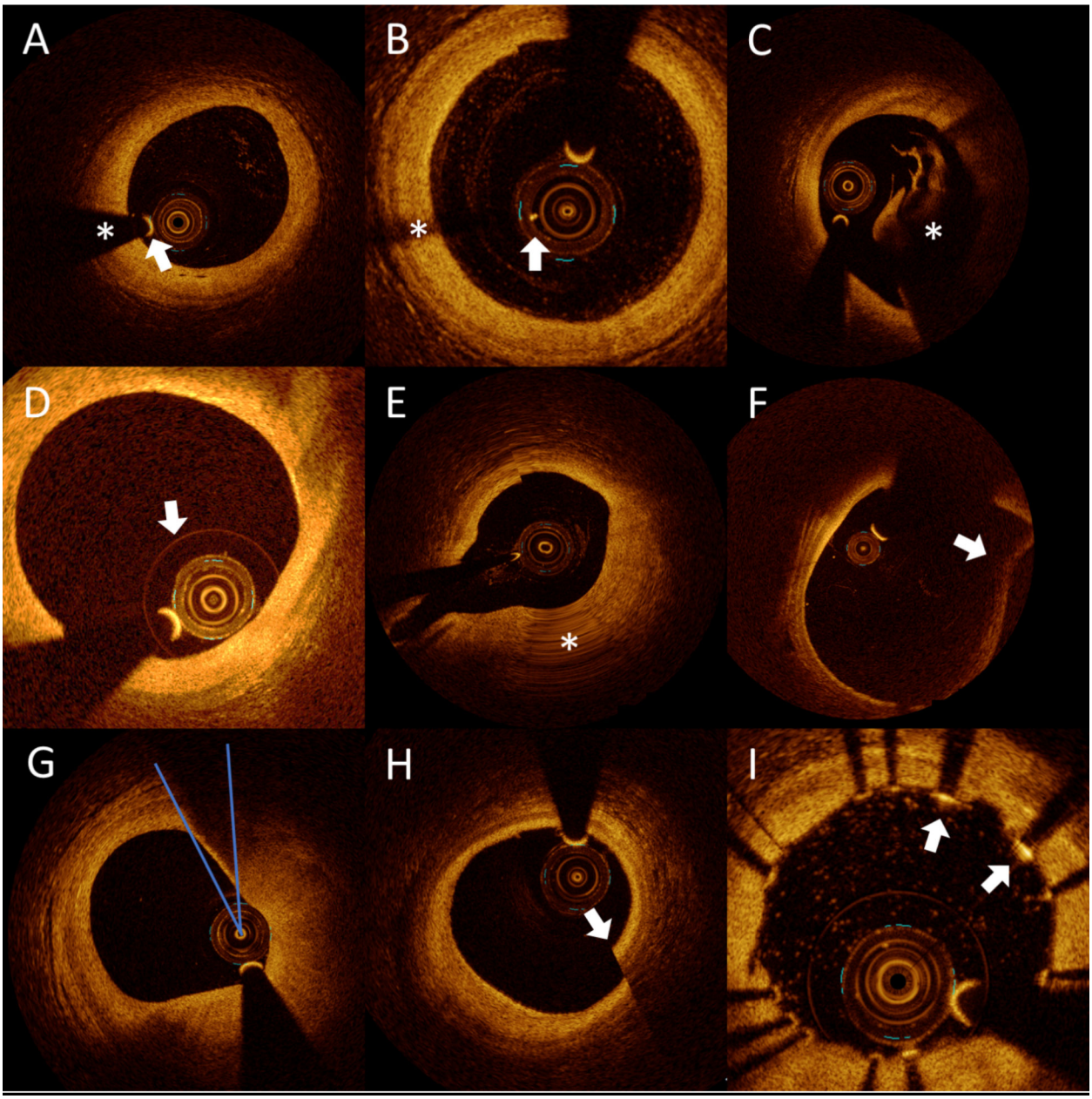

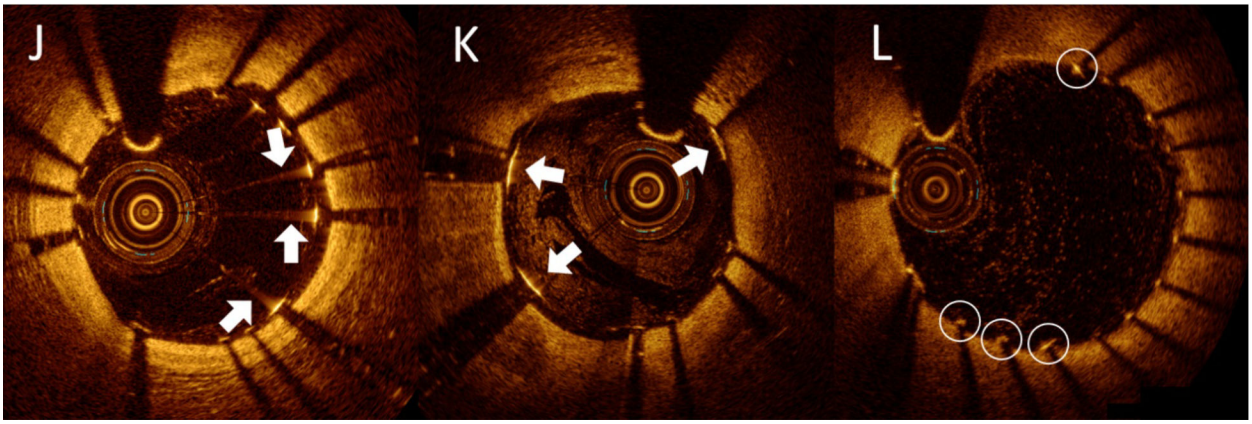

Figure 1. Artifacts

(A) Guide wire (arrow) causes a shadow (asterisk). (B) Gas bubbles in the catheter (arrow) cause a shadow (asterisk). (C) Suboptimal vessel flushing leads to residual blood in the lumen (asterisk), hampering the assessment of the vessel (D) Ghost lines (arrow). (E) Non-uniform rotational distortion (NURD) (asterisk). (F) Fold-over artifact (arrow). (G) Tangential signal dropout. Blue lines indicate the direction of light beams tangential to the tissue that appears to have an artifactual light dropout. (H) Seam artifact (arrow). (I) Blooming. Stent struts (arrows) appear thicker than the actual thickness due to blooming artifact. (J) Saturation. Arrows point to high signal intensity artifact that extends along the axial dimension. (K) Merry-go-round artifact is artifactual stretching in the lateral (rotational) direction of stent struts (arrows), which occurs due to scatters in the lumen such as residual blood, clots and neointima. (L) Sunflower artifact may cause a well-apposed stent to appear malapposed in a vessel (white circles).

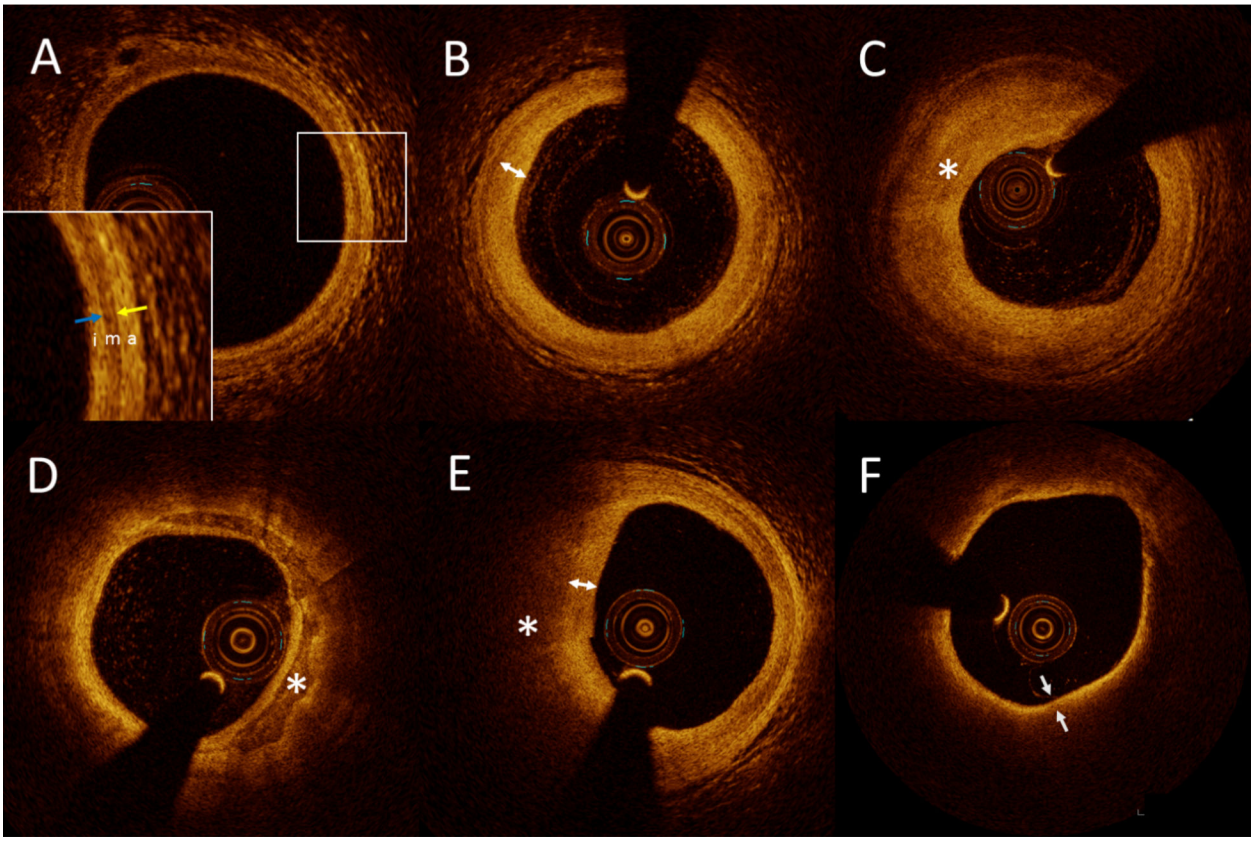

Figure 2. Normal vessel and plaques

(A) Normal vessel wall is characterized by 3-layered architecture, comprising a high backscattering, thin intima (i), a low backscattering media (m), a high backscattering adventitia (a), internal elastic membrane as the border between the intima and media (blue arrow), and external elastic membrane as the border between the media and the adventitia (yellow arrow). (B) Intimal thickening occurs during the early phase of atherosclerosis in the coronary artery, which is represented as a signal-rich thick intimal band (double-headed arrow). (C) Fibrous plaque exhibits homogeneous, signal-rich (highly backscattering) regions (asterisk). (D) Calcified plaque exhibits signal-poor regions with sharply delineated borders and limited shadowing (asterisk). (E) Lipid plaque exhibits signal-poor regions (asterisk) with diffuse borders and overlying signal-rich bands (double-headed arrow). (F) Thin-cap fibroatheroma (TCFA) is defined as a lipid plaque in which the minimum thickness of the fibrous cap (arrows) is less than a predetermined threshold and lipid occupies >90° in circumference.

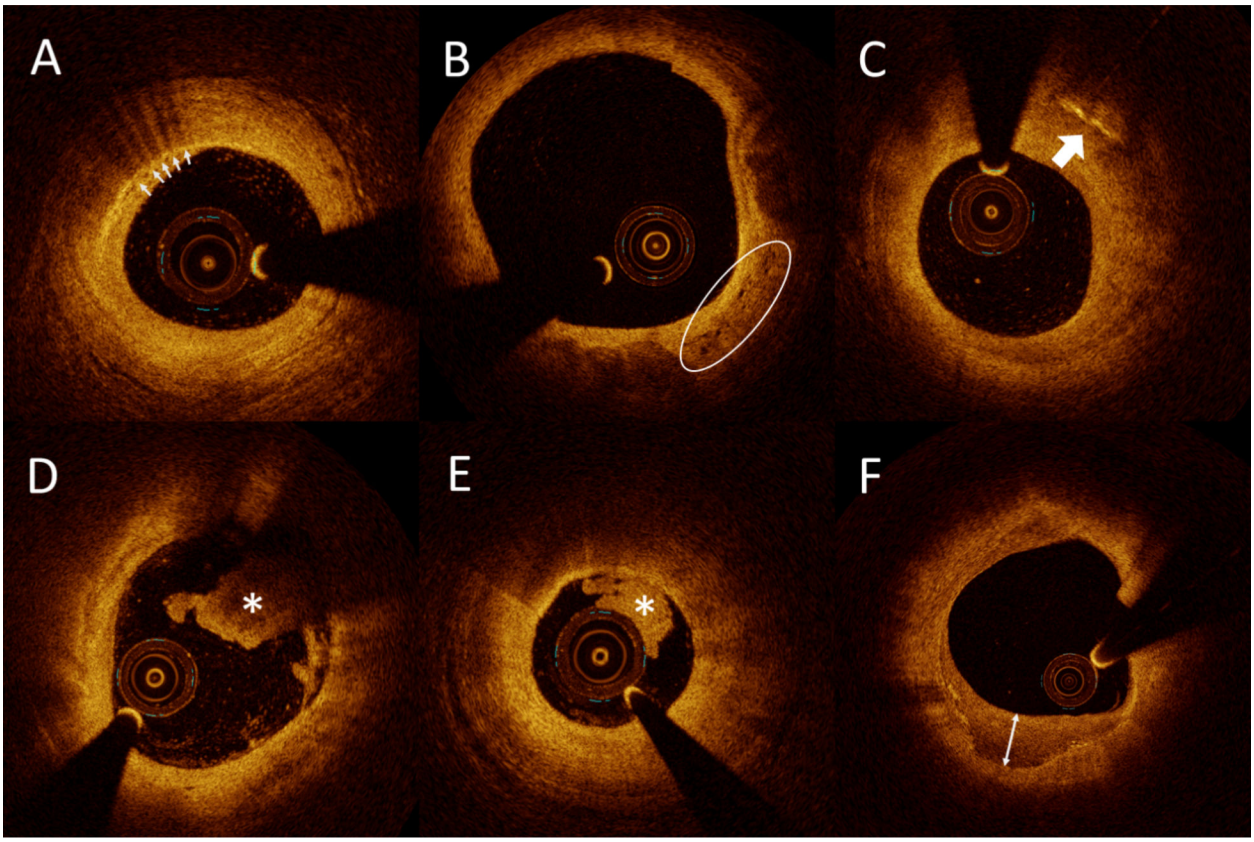

Figure 3. Qualitative findings

(A) Macrophages are seen as signal-rich, distinct, or confluent punctate regions that exceed the intensity of background speckle noise and cast a dark shadow (arrows). (B) Microvessels within the intima can appear as signal-poor voids that are sharply delineated and can usually be followed in multiple contiguous frames (white circle). (C) Cholesterol crystals appear as thin, linear regions of high intensity (arrow), usually in proximity to a lipid-rich plaque. (D) Thrombus is seen as an irregular mass protruding into the lumen. Red thrombus is seen as a high backscattering protrusion with signal-free shadowing (asterisk). (E) White thrombus is seen as a signal-rich, low backscattering projection, which does not obscure the vessel (asterisk). (F) Layered plaque. The double-headed arrow indicates a layer of different optical densities.

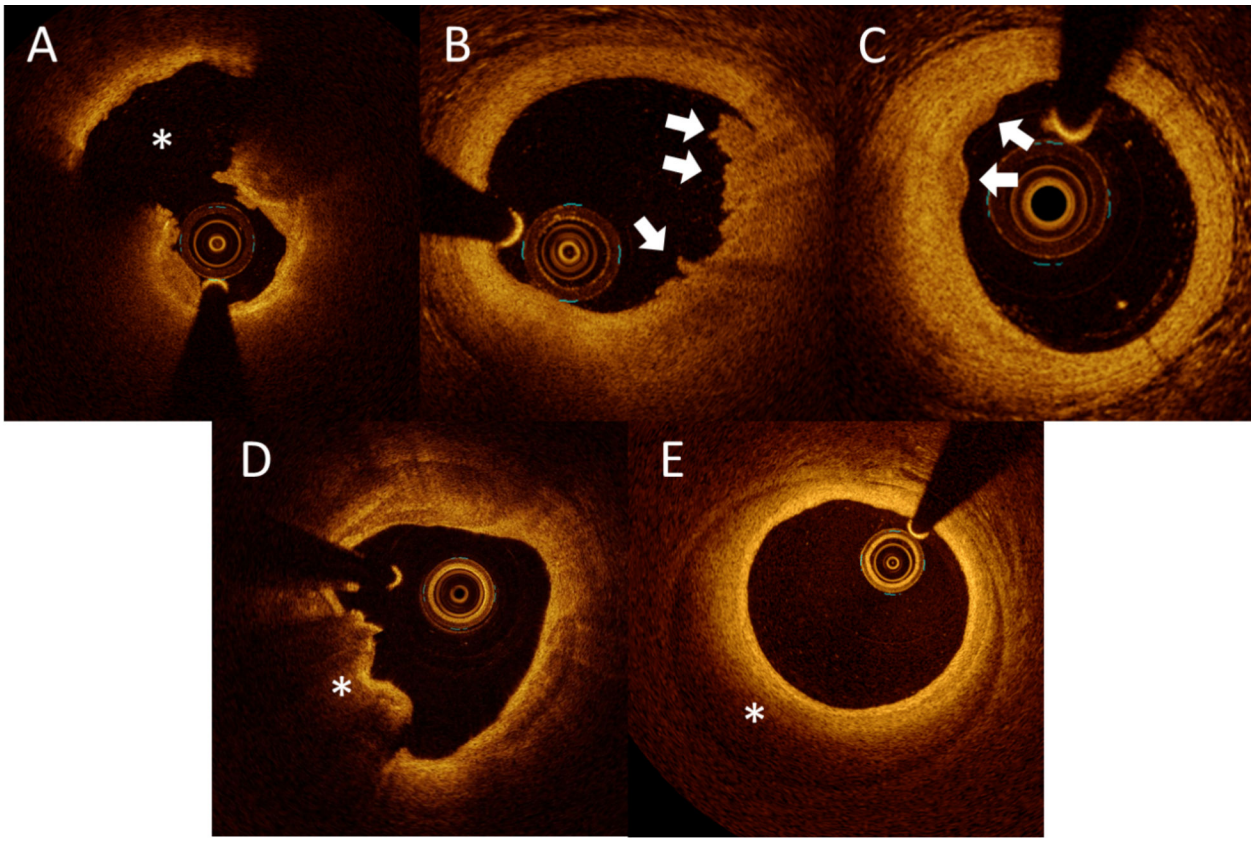

Figure 4. Culprit lesions in ACS patients

(A) Plaque rupture is characterized by the presence of fibrous cap discontinuity with a cavity formation (asterisk) within the plaque. (B) Definite erosion is characterized by the presence of attached thrombus (arrows) overlying an intact and visualized plaque. (C) Probable erosion is characterized by luminal surface irregularity (arrows) at the culprit lesion in the absence of thrombus. (D) Eruptive calcified nodule appears in OCT as single or multiple regions of calcium that protrude into the lumen with fibrous cap disruption, frequently forming sharp, protruding edges, and the presence of substantive calcium proximal and/or distal to the lesion (asterisk). (E) Spontaneous coronary artery dissection (SCAD) is seen as a separation of the intima and media from the adventitia (intramural hematoma) (asterisk), with or without communication with the vessel lumen (intimal tear). ACS = acute coronary syndrome

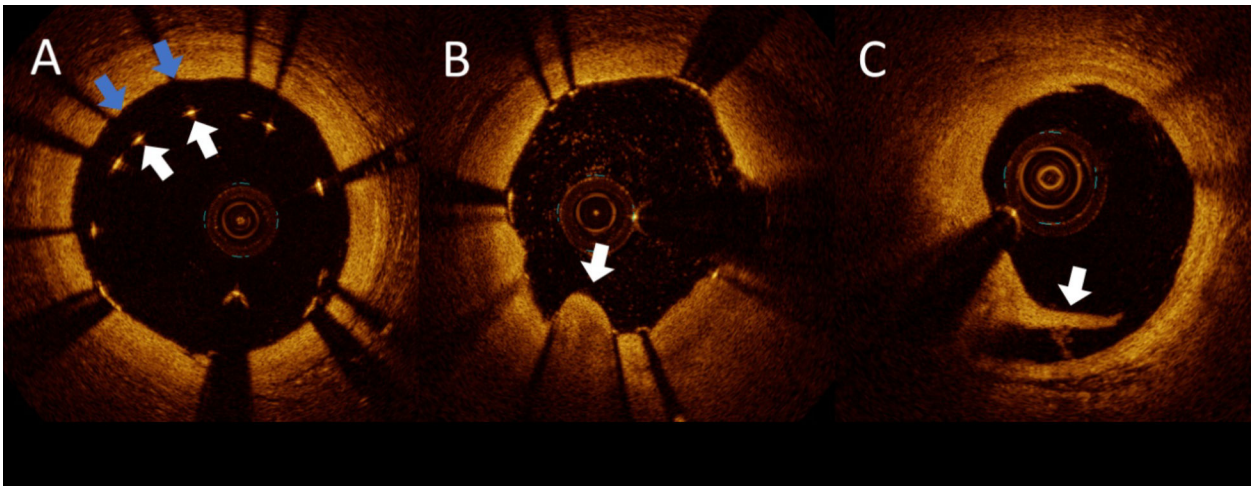

Figure 5. Post-PCI findings

(A) Strut malapposition. Stent struts (white arrows) are distant from the luminal surface of the artery wall (blue arrows). (B) Tissue prolapse is a tissue extrusion from inside the stent area (arrow). (C) Edge dissection (arrow).

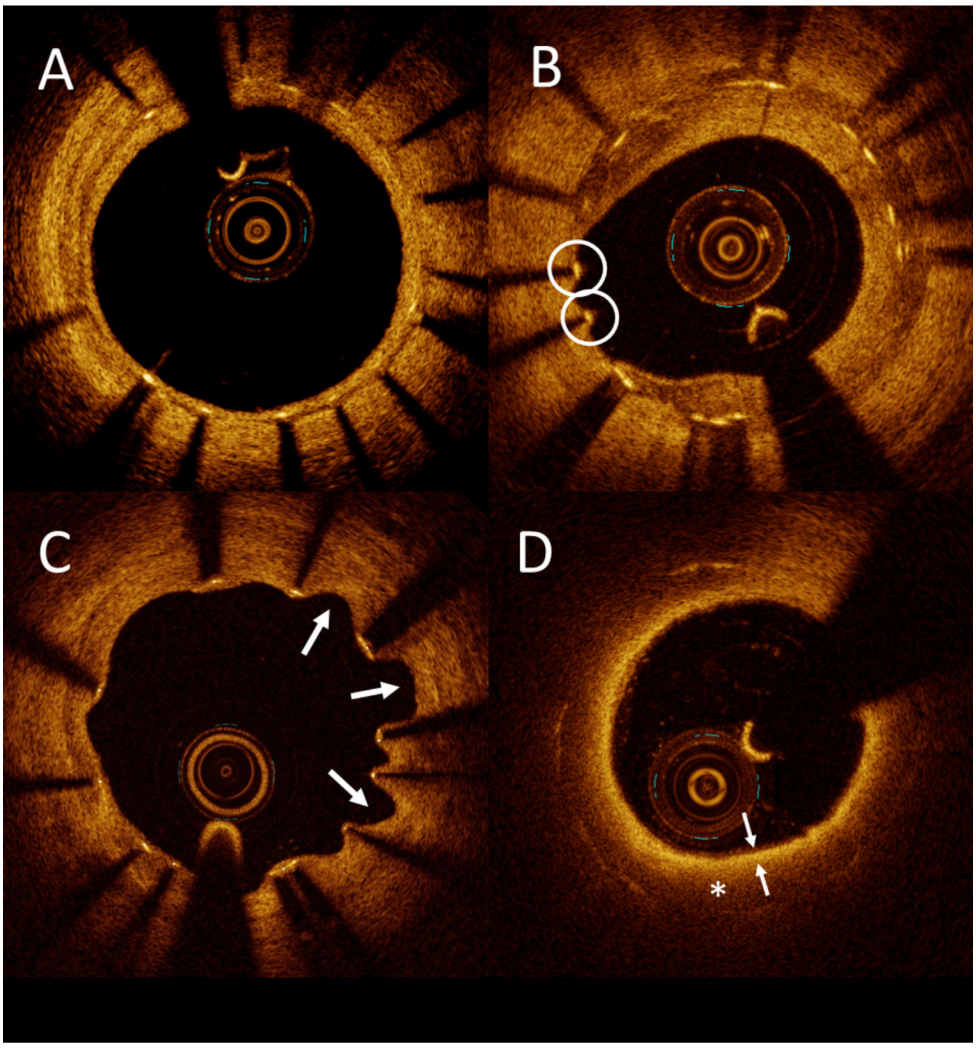

Figure 6. Vascular response after stenting

(A) Covered struts. Stent struts are considered covered when tissue can be identified on the luminal side of the strut. (B) Uncovered struts. Struts are considered uncovered when tissue cannot be identified above the strut (struts in white circles). (C) Evagination. An outward bulge (arrows) in the luminal vessel contour between apposed struts. (D) Neoatherosclerosis. A signal-poor region with a diffuse border (asterisk) and an overlying signal-rich band (arrows), which correspond with lipid-laden tissue is seen within the stent.

Table 1.

Summary of OCT artifacts

Names	Characteristics
Guide wire	An artifact that is present in all current clinical OCT images is a sharp shadow caused by the guide wire. The guide wire will block the OCT light beam, so that tissue and stents behind the wire cannot be imaged (Figure 1A).
Gas bubbles	Gas bubbles can be present inside fluid-filled catheters. They can be recognized as distinct focal bright regions inside the catheter and a diminished signal in the part of the OCT image in the path of the affected region of the catheter (Figure 1B). These gas bubbles can form inside the OCT catheter if the operator does not adequately flush the catheter before introduction into the guide. Gas bubbles can also appear in the lumen of the vessel, injected through
Suboptimal vessel flushing	When blood is inadequately cleared from the field of the view, amorphous bright features can be present in the OCT image, because erythrocytes scatter light (Figure 1C). When mixed with optically transparent flushing media, blood may form many different patterns within the artery lumen. Blood can be confused with red thrombus or vessel wall dissections. Care should be taken when performing measurements and interpreting plaque components and stents through blood, as blood attenuates the OCT signal and therefore
Ghost lines	Ghost lines appear as circular features around the OCT catheter in the OCT image (Figure 1D). These lines appear in the image but are caused by light reflections from interfaces within the catheter or optical connections between OCT instrument and catheter. These artifacts should be identified and not interpreted as the OCT catheter sheath. If the ghost lines are misinterpreted and used for a calibration, measurements will be artifactually reduced. For
Non-uniform rotational distortion (NURD)	NURD is due to variations in the rotation rate of the catheter torque cable and distal optics and appears in OCT images as a blurring or smearing in the lateral (or rotational) direction (Figure 1E). NURD is normally caused by mechanical rotational resistance in the catheter due to either a tortuous or narrow vessel, a
Fold-over artifact	When the vessel diameter is larger than the ranging depth, a portion of the vessel may appear to fold over in the image (Figure 1F). These portions of the image data that contain fold-over artifacts should not be interpreted.
Tangential signal dropout	When the catheter is located very eccentrically, near the vessel wall, the optical beam may be directed almost parallel to the tissue surface. In these situations, the light beam is attenuated as it passes along the surface of the artery wall and the resultant artery wall may appear signal-poor below the luminal surface (Figure 1G). This artifact may be confused with the appearance of a thin-capped fibroatheroma (TCFA), intimal disruption, or
Seam artifact	If the catheter has moved with respect to the vessel during the time of single cross-sectional image acquisition, an axial discontinuity termed a seam artifact (Figure 1H), may appear at the location of the transition between the first and
Blooming	Blooming is the increase in strut reflection thickness in the axial direction of OCT images (Figure 1I), causing the small bright-line segment that represents the leading edge of a stent strut to appear thicker than normal, making it
Saturation	When a high reflector is encountered by OCT light, it may be backscattered at too high an intensity to be accurately detected by the detector, thereby causing saturation artifact (Figure 1J). Structures that exhibit high backscattering commonly include the guide wire, the tissue surface, and metallic stent struts.
Merry-go-round artifact	Merry-go-round artifact occurs when the small bright-line segments that represent a stent strut appear elongated in the lateral (rotational) direction (Figure 1K). Merry-go-rounding has also been described as an artifactual stretching of the stent strut. It is proposed that optical scattering in the lumen (primarily due to inadequate blood flushing) between the catheter and arterial
Sunflower artifact	When the OCT catheter is eccentrically located in the presence of metallic stent struts, a sunflower artifact can occur. Sunflower artifact occurs when stent struts appear to curve towards the OCT catheter, like sunflowers growing toward the sun (Figure 1L). This artifact may cause a well-apposed stent to appear malapposed in a vessel. This occurs because incident OCT light only